

Lawrence Berkeley National Laboratory

LBL Publications

Title

Systematic and scalable genome-wide essentiality mapping to identify nonessential genes in phages.

Permalink

<https://escholarship.org/uc/item/0k73m30p>

Journal

PLoS Biology, 21(12)

Authors

Piya, Denish

Nolan, Nicholas

Moore, Madeline

et al.

Publication Date

2023-12-01

DOI

10.1371/journal.pbio.3002416

Peer reviewed

METHODS AND RESOURCES

Systematic and scalable genome-wide essentiality mapping to identify nonessential genes in phages

Denish Piya¹, Nicholas Nolan², Madeline L. Moore³, Luis A. Ramirez Hernandez³, Brady F. Cress^{1,4}, Ry Young⁵, Adam P. Arkin^{1,2,3*}, Vivek K. Mutalik^{1,3*}

1 Innovative Genomics Institute, University of California-Berkeley, Berkeley, California, United States of America, **2** Department of Bioengineering, University of California-Berkeley, Berkeley, California, United States of America, **3** Environmental Genomics and Systems Biology Division, Lawrence Berkeley National Laboratory, Berkeley, California, United States of America, **4** Department of Molecular and Cell Biology, University of California-Berkeley, Berkeley, California, United States of America, **5** Department of Biochemistry and Biophysics, Center for Phage Technology, Texas A&M University, College Station, Texas, United States of America

* aparkin@lbl.gov (APA); vkmutalik@lbl.gov (VKM)

OPEN ACCESS

Citation: Piya D, Nolan N, Moore ML, Ramirez Hernandez LA, Cress BF, Young R, et al. (2023) Systematic and scalable genome-wide essentiality mapping to identify nonessential genes in phages. *PLoS Biol* 21(12): e3002416. <https://doi.org/10.1371/journal.pbio.3002416>

Academic Editor: Paula Jauregui, PhD, PLOS: Public Library of Science, UNITED KINGDOM

Received: May 23, 2023

Accepted: November 2, 2023

Published: December 4, 2023

Peer Review History: PLOS recognizes the benefits of transparency in the peer review process; therefore, we enable the publication of all of the content of peer review and author responses alongside final, published articles. The editorial history of this article is available here: <https://doi.org/10.1371/journal.pbio.3002416>

Copyright: © 2023 Piya et al. This is an open access article distributed under the terms of the [Creative Commons Attribution License](https://creativecommons.org/licenses/by/4.0/), which permits unrestricted use, distribution, and reproduction in any medium, provided the original author and source are credited.

Data Availability Statement: All relevant data are within the paper and its [Supporting Information](#) files. The underlying data for all figures are provided in [supporting information](#) file [S1 Data](#).

Abstract

Phages are one of the key ecological drivers of microbial community dynamics, function, and evolution. Despite their importance in bacterial ecology and evolutionary processes, phage genes are poorly characterized, hampering their usage in a variety of biotechnological applications. Methods to characterize such genes, even those critical to the phage life cycle, are labor intensive and are generally phage specific. Here, we develop a systematic gene essentiality mapping method scalable to new phage–host combinations that facilitate the identification of nonessential genes. As a proof of concept, we use an arrayed genome-wide CRISPR interference (CRISPRi) assay to map gene essentiality landscape in the canonical coliphages λ and P1. Results from a single panel of CRISPRi probes largely recapitulate the essential gene roster determined from decades of genetic analysis for lambda and provide new insights into essential and nonessential loci in P1. We present evidence of how CRISPRi polarity can lead to false positive gene essentiality assignments and recommend caution towards interpreting CRISPRi data on gene essentiality when applied to less studied phages. Finally, we show that we can engineer phages by inserting DNA barcodes into newly identified inessential regions, which will empower processes of identification, quantification, and tracking of phages in diverse applications.

Introduction

Bacteriophages (phages) are the most abundant biological entities on earth and are postulated to play a crucial role in environmental nutrient cycles, agricultural productivity, and human health [1,2]. The full scope of the roles phages play in regulating the activity and adaptation of microbial communities is still emerging [3–5]. Phages represent one of the largest pools of genetic diversity with unexplored functional information [6–9]. For example, the majority of

The complete data from phage Barseq experiments are deposited here <https://doi.org/10.6084/m9.figshare.22817084>.

Funding: This material by ENIGMA- Ecosystems and Networks Integrated with Genes and Molecular Assemblies (<http://enigma.lbl.gov>), a Science Focus Area Program at Lawrence Berkeley National Laboratory is based upon work supported by the U.S. Department of Energy, Office of Science, Office of Biological & Environmental Research under contract number DE-AC02-05CH11231 (to V.K.M. and A.P.A.). Phage P1 assay part of this research was supported by the U.S. Department of Energy, Office of Science, through the National Virtual Biotechnology Laboratory, a consortium of U.S. Department of Energy national laboratories focused on response to COVID-19, with funding provided by the Coronavirus CARES Act (to V.K.M. and A.P.A.) and the early design part of this project was funded by the Microbiology Program of the Innovative Genomics Institute, Berkeley (to A.P.A. and V.K.M.). R.F.Y. acknowledges funding from the National Institute of General Medical Sciences (NIGMS) grant R35GM136396. The funders had no role in study design, data collection and analysis, decision to publish, or preparation of the manuscript.

Competing interests: V.K.M., D.P. and A.P.A. are holders of a patent (pending) on the phage barcoding technology. V.K.M. is a co-founder of Felix Biotechnology. A.P.A. is a co-founder of Boost Biomes and Felix Biotechnology. A.P.A. is a shareholder in and advisor to Nutcracker Therapeutics. The remaining authors declare no competing interests.

Abbreviations: aTc, anhydrotetracycline; CRISPRi, CRISPR interference; crRNA, CRISPR RNA; EOP, efficiency of plating; Lpa, Late Promoter Activator; ORF, open reading frame; PAM, protospacer adjacent motif.

phage genes (>70% to 80%) identified by bioinformatic analysis are of unknown function and show no sequence similarity to characterized genes [10]. Homology-based approaches to connect phage genes to their function are limited by the lack of experimental data [11,12]. While focused biochemical and genetic analysis are the gold standard for assessment of gene functions, most of these methods are not scalable to the vast amount of new genes being discovered [10]. Unless we develop methods to fill the knowledge gap between phage genetic diversity and gene function, we will be seriously constrained in understanding the mechanistic ecology of phages in diverse microbiomes and harness them as engineerable antimicrobials and microbial community editors [13,14].

Gaps in phage gene-function knowledge exist even for some of the most well-studied canonical phages [15,16]. Nevertheless, the application of classical phage genetic tools to a few canonical phages over the last few decades has paved the way for generating foundational knowledge of the phage life cycle [15,17,18]. A number of recent technological innovations have also addressed the growing knowledge gap between phage-gene-sequence and the encoded function [19–21]. These innovations range from classical recombineering methods [22,23] and new phage engineering platforms [24–28] to genome editing tools such as CRISPR systems, with or without recombineering technology to create individual phage mutants [13,25,29–33]. Importantly, no method for assessing essentiality without genome modification has been reported. As such, the field is in need of genome-wide technologies that can be used rapidly across diverse phages to assess gene function [14]. At minimum, such a method would provide the foundational knowledge of which phage genes are essential for its infection cycle in a given host, a prerequisite for understanding host range and for engineering.

Catalytically inactive CRISPR RNA (crRNA)-directed CRISPR endonucleases or CRISPR interference (CRISPRi) technology has emerged as a facile tool for carrying out genome-scale targeted interrogation of gene function in prokaryotic and eukaryotic cells without modification of the genome [34,35]. A catalytically inactive or “dead” Cas protein (such as dCas9 or dCas12a) enables programmable transcriptional knockdown (by binding to DNA and forming a transcriptional road block) yielding a loss-of-function phenotype in a DNA sequence-dependent manner [36–41]. While CRISPRi was first developed using dCas9, alternative Cas variants like dCas12a have achieved efficient knockdown in diverse bacteria [42–44]. Both dCas9 and dCas12a are similarly effective for CRISPRi in many circumstances; however, advantages of dCas12 include more efficient restriction of a covalently modified phage genome (for example, T4 phage [45]) and simpler cloning of dual crRNAs on short oligos relative to longer dCas9 single-guide RNAs. Recent work demonstrated that dCas12a is capable of inhibiting infection by phage λ when targeting the essential gene *cro*, suggesting that application of dCas12a with arrayed crRNAs might facilitate genome-wide fitness measurements in phages [46]. The ability to effectively block transcription at target sites distant from promoters makes dCas12a potentially well suited for repressing transcription of phage genes within operons that show overlapping genetic architecture [15,17,18,47,48] and those that are highly regulated or vary in expression levels [49–51] in a noncompetitive plaque assay.

Here, we adopted catalytically inactive Cas12a (dCas12a) to carry out systematic genome-wide interference assays in 2 canonical phages. The first is coliphage lambda, arguably the best characterized virus in terms of individual gene function and developmental pathways [17]. The second is coliphage P1, which, as a powerful generalized transducing phage, was instrumental in the development of *Escherichia coli* as a primary genetic model [52]. Its genome is also well annotated but less experimentally characterized than lambda. We first benchmark the CRISPRi technology by applying it to a known set of essential and nonessential genes in both phages (lytic variants, λ C1857, and P1vir, here onwards as lambda or λ and P1, respectively) and then extend it genome-wide to query essentiality of all genes in both phages. Although

some ambiguities are revealed and significant polarity effects are detected, the method is clearly demonstrated to be applicable to the rapid assignment of nonessential loci in phages, thus paving the way for systematic genome-scale engineering in a variety of applications.

Results

Setting up CRISPRi assay targeting phage genes

To ascertain that dCas12a can repress phage gene expression, we designed a phage targeting CRISPRi plasmid system following earlier work [53] by expressing both dCas12a and a crRNA to target specific genes (Methods). Briefly, we placed dCas12a under an anhydrotetracycline (aTc)-inducible Tet promoter and the CRISPR array including the phage targeting crRNA under a strong constitutive promoter on a medium copy plasmid. We then selected a set of known essential and nonessential genes that encode proteins needed at different copy numbers for lambda and P1 (Fig 1). For lambda, we chose *E*, which encodes the major capsid protein, and *Nu1*, which encodes the small terminase subunit. For P1, we chose genes 23, *pacA*, and *sit*, encoding the major capsid protein, large terminase subunit, and tape measure protein, respectively [17,52]. In addition to these essential phage genes, we also chose nonessential P1 genes such as *ppp*, *upfB*, or *ddrB* [54]. We identified Cas12a protospacer adjacent motif (PAM) sites (TTTV) in the 5' end of the genes (approximately 20% downstream of the start site) and used 28 bp nucleotide sequence immediately downstream of the PAM site in the coding strand as the spacer region for designing crRNAs.

We performed plate-based CRISPRi efficiency assays by moving each variant of the CRISPRi plasmid into *E. coli* BW25113 separately and induced the expression of dCas12a before plating serial dilution of the 2 phages (Methods). After overnight incubation, we compared the plating efficiency on lawns expressing the gene-targeting crRNAs versus a control lawn in which the crRNA did not target either phage (Fig 1B). We observed that induction of CRISPRi targeting essential genes *E* and *nu1* of lambda and *mcp*, *pacA*, and *sit* of P1 all showed severe compromise in phage growth (measured as plaque formation), whereas targeting nonessential genes *ppp*, *upfB*, or *ddrB* of P1 did not. Overall, our CRISPRi benchmarking assays indicated that the dCas12a CRISPRi platform can be used to assess essentiality of phage genes expressed at different levels during the infection cycle.

Genome-wide CRISPRi to map gene essentiality in λ

To extend our initial observations to systematically query gene essentiality at genome-wide levels, we considered λ as our pilot case, since it is the most deeply characterized phage with detailed assessments of gene functions well represented in the literature [17,55]. Decades of work on suppressible nonsense mutants of λ phage have helped to define 28 genes (out of total 73 open reading frames (ORFs)) as essential for phage growth (Table 1) providing a well-characterized test bed for validation of our genome-wide CRISPRi assay.

We designed individual crRNAs targeting 67 out of 73 genes of the lambda genome, using the same criteria as used for the pilot studies (by locating PAM sites in the 20% to 33% of the way through the CDS region of each gene to account for any possible alternative start sites for genes) (S1 Fig). The remaining 6 genes (*cII*, *ninD*, *ninE*, *ninH*, *Rz1*, and *lambdap35*) were not tested here due to lack of canonical PAM sites. The designed crRNAs were synthesized as separate pairs of oligos and cloned into the CRISPRi plasmid system downstream of a strong constitutive promoter (Methods). Each of these plasmids encoding crRNAs were arranged in an arrayed format and moved into *E. coli* BW25113 as indicator strains for the plate-based CRISPRi assay to measure the efficiency of plating (EOP) (Fig 2, described above, and Methods). The EOP is a quantitative measure of the knockdown for each guide RNA. We assessed the

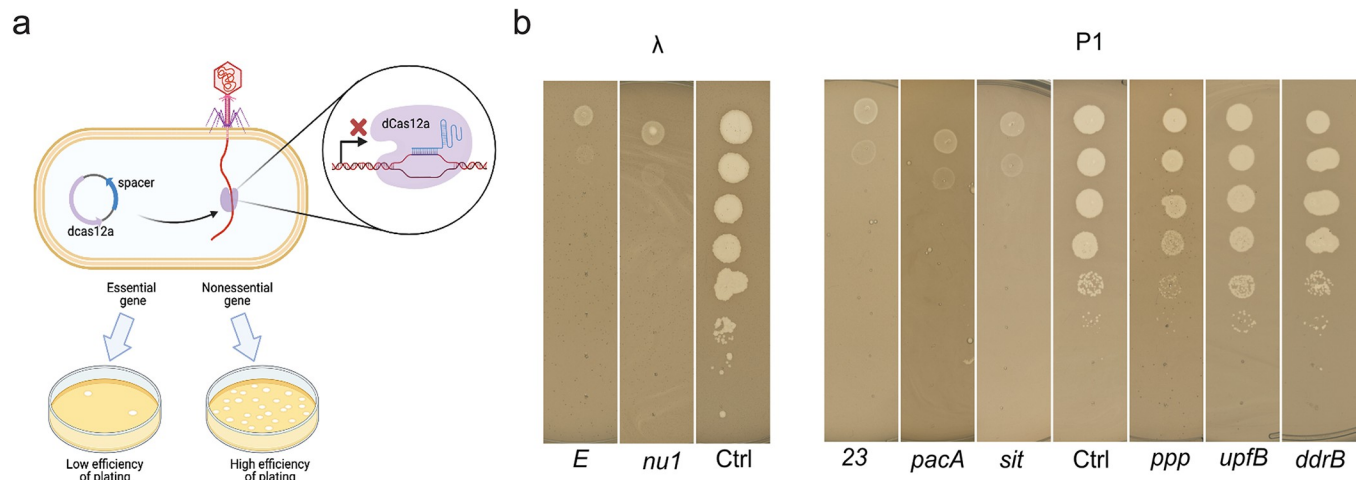


Fig 1. Design and testing of CRISPRi knockdowns to assess gene essentiality in phages lambda and P1. (a) Schematic of CRISPRi assay system. (b) Representative images of plaque assays to validate the dCas12a CRISPRi system using gene targets with known essentiality. We employed crRNAs targeting 2 essential genes of phage λ : genes encoding major capsid protein (E) or DNA packaging subunit (Nu1). For phage P1, we used crRNA targeting 3 essential genes: encoding the major capsid protein (gene 23 encoding Mcp), DNA packaging subunit (PacA), and tape measure protein (Sit); and 3 nonessential genes: *ppp*, *upfB*, or *ddrB*. For comparison, phage plaques appearing on an *E. coli* BW25113 lawn expressing a nontargeting crRNA as a control are shown for both phages (Ctrl).

<https://doi.org/10.1371/journal.pbio.3002416.g001>

reproducibility of EOP estimations by carrying out biological replicates (total assays >150) and depicted the average EOP of every gene on the lambda map (Fig 3 and Table 1, Note A in S1 Text).

In total, our CRISPRi assays indicated 35 genes as essential and 32 genes as nonessential. For example, consistent with the literature [17], knockdown of genes that encode factors involved in the structural assembly of λ virions, either the capsid morphogenesis (Nu1, A, B, C, Nu3, D, E, Fl) or tail morphogenesis (V, G, G-T, H, M, L, K, I, J), were detrimental to phage growth with 5-log reduction in EOP. Similarly, repression of genes encoding crucial factors involved in the lytic phase of lambda phage growth cycle, such as transcription antiterminators (proteins N and Q), DNA replication (proteins O and P), transcriptional regulator (Cro), and programmed disruption of host membrane (holin/antiholin S and S') all showed approximately 4- to 5-log reduction in EOP, indicating their important role in phage fitness phenotype (Table 1).

The longest stretch of dispensable DNA for lambda encompasses >30% of its genome and is made up of 4 clusters of genes arranged between gene J and gene N (Fig 3). These include a cluster of genes *lom-stf-tfa*, 20 genes within pL operon, genes in the immunity region (*rex* and *cI* genes), and genes encoding the lysis program (*R* and *Rz*). We found, except for gene N, all genes within pL operon are dispensable for lambda plaque formation (Fig 3 and Table 1). Some of these genes provide functions that would not be expected to have a plaque-formation defect on fully competent lawns, like the superinfection exclusion genes (*rexA*, *rexB*, *sieB*) [56] and genes involved in lysogeny (*int*, *xis*, *CIII*) [57], but others might, such as homologous recombination (*exo*, *bet*, *gam*) [58] and inhibition of host cell division (*kil*) [59]. The knockdown of *ral* (encoding a restriction inhibitor protein) does not result in a major defect in the EOP because our indicator strain lacks a functional type I restriction system [60,61]. To probe the essentiality of *ral*, we repeated the knockdown assays on 2 different strains with active type I restriction system (Methods). These assays indicate the conditional essentiality of *ral* that depends on the genotype of the target bacterial strain (S2 Fig). The dispensability of the side tail fiber (which requires *stf* and *tfa*) is in agreement with the known frameshift mutation in the *stf* locus in laboratory strains of λ [62]

Table 1. Gene essentiality mapping of phage lambda genome.

Locus_tag	Gene	function/Protein name [17]	EOP_average	S.D.	This work	Literature
lambdap01	<i>nu1</i>	DNA packaging protein	5.5E-06	2.1E-06	E	E [91]
lambdap02	<i>A</i>	TerL	1.3E-06	4.7E-07	E	E [92,93]
lambdap03	<i>W</i>	gpW family protein	3.0E-05	1.4E-05	E	E [93,94]
lambdap04	<i>B</i>	portal	2.5E-05	2.1E-05	E	E [92,93]
lambdap05	<i>C</i>	S49 family peptidase/capsid component; Viral protease	<2.0E-7		E	E [93,95]
lambdap06	<i>nu3</i>	scaffolding protein	<2.0E-7		E	E [93,96]
lambdap07	<i>D</i>	head decoration protein	6.8E-06	2.4E-07	E	E [93,97]
lambdap08	<i>E</i>	major capsid protein	<6.4E-6		E	E [93,97]
lambdap09	<i>Fi</i>	DNA packaging protein FI	2.0E-05	0.0E+00	E	E [93,98]
lambdap10	<i>Fii</i>	head-tail joining protein	<2.0E-7		E	E [94]
lambdap11	<i>Z</i>	tail protein	2.5E-05	7.1E-06	E	E [55]
lambdap12	<i>U</i>	tail protein	3.5E-05	2.1E-05	E	E [55]
lambdap13	<i>V</i>	tail protein	1.7E-05	1.9E-05	E	E [55]
lambdap14	<i>G</i>	minor tail protein G	<6.4E-6		E	E [99]
lambdap15	<i>T</i>	tail assembly protein T	1.2E-05	1.2E-05	E	E [99]
lambdap16	<i>H</i>	tail tape measure protein	1.0E-06	9.4E-07	E	E [99]
lambdap17	<i>M</i>	tail protein	<2.0E-7		E	E [99]
lambdap18	<i>L</i>	minor tail protein L	<2.0E-7		E	E [99]
lambdap19	<i>K</i>	tail protein	8.7E-05	1.2E-04	E	E [99]
lambdap20	<i>I</i>	tail component	2.6E-05	2.7E-05	E	E [100]
lambdap21	<i>J</i>	host specificity protein J	1.1E-05	1.2E-05	E	E [92]
lambdap26	<i>lom</i>	Outer membrane beta-barrel protein Lom	8.8E-01	5.3E-01	NE	NE [17]
lambdap27	<i>stf</i>	protail fiber N-terminal domain containing protein	3.0E+00	2.8E+00	NE	NE [62]
lambdap90	<i>orf206b</i>	hypothetical protein	4.3E+00	1.1E+00	NE	NE [62]
lambdap28	<i>tfa</i>	tail fiber protein	6.3E+00	5.3E+00	NE	NE [62]
lambdap29	<i>orf-194</i>	tail fiber assembly protein	3.3E+00	1.1E+00	NE	NE [62]
lambdap80	<i>ea47</i>		5.5E+00	6.4E+00	NE	NE [17]
lambdap81	<i>ea31</i>		1.2E+00	1.1E+00	NE	NE [17]
lambdap82	<i>ea59</i>	ATP-dependent endonuclease	1.3E+01	1.7E+01	NE	NE [17]
lambdap33	<i>int</i>	tyrosine-type recombinase/integrase	2.8E+00	3.2E+00	NE	NE [55]
lambdap34	<i>xis</i>	excisionase	1.6E+00	1.1E+00	NE	NE [55]
lambdap35					NT	
lambdap36	<i>ea8.5</i>		1.4E+00	1.3E+00	NE	NE [17]
lambdap83	<i>ea22</i>	ead/Ea22-like family protein	2.2E+00	2.3E+00	NE	NE [17]
lambdap37	<i>orf61</i>	hypothetical protein	9.7E-01	8.1E-01	NE	NE [17]
lambdap38	<i>orf63</i>	DUF1382 family protein	1.3E+00	3.8E-01	NE	NE [17]
lambdap39	<i>orf60a</i>	DUF1317 domin-containing protein	2.4E+00	2.0E+00	NE	NE [17]
lambdap41	<i>exo</i>	YqaJ viral recombinase family protein	6.9E-01	4.4E-01	NE	NE [17]
lambdap84	<i>bet</i>	recombination protein Bet	2.1E+00	2.5E+00	NE	NE [17,101]
lambdap42	<i>gam</i>	host-nuclease inhibitor protein Gam	1.4E+00	1.3E+00	NE	NE [17,101]
lambdap85	<i>kil</i>	host cell division inhibitory peptide Kil	1.0E+00	0.0E+00	NE	NE [102]
lambdap86	<i>cIII</i>	protease FtsH-inhibitory lysogeny factor CIII	1.1E+00	3.1E-01	NE	NE [103,104]
lambdap45	<i>ea10</i>	DUF2528 family protein	1.7E+00	4.7E-01	NE	NE [17]
lambdap46	<i>ral</i>	Restriction inhibitor protein ral	1.1E+00	3.2E-01	NE	NE [60,61]
lambdap47	<i>orf28</i>	hypothetical protein	1.3E+00	4.7E-01	NE	NE [17]
lambdap48	<i>sieB</i>	Superinfection exclusion protein B	1.5E+00	7.1E-01	NE	NE [105]
lambdap49	<i>N</i>	antitermination protein N	1.8E-04	1.2E-04	E	E [106,107]

(Continued)

Table 1. (Continued)

Locus_tag	Gene	function/Protein name [17]	EOP_average	S.D.	This work	Literature
lambdap53	<i>rexB</i>	exclusion protein	1.4E+00	1.3E+00	NE	NE [17,105]
lambdap87	<i>rexA</i>	exclusion protein	3.8E+00	4.0E+00	NE	NE [17,105]
lambdap88	<i>cl</i>	lysogenic repressor	5.3E+00	6.6E+00	NE	NE [103,108,109]
lambdap57	<i>cro</i>	lytic repressor	<7.5E-6		E	E [110]
	<i>cII</i>				NT	NE [103,108,109]
lambdap89	<i>O</i>	replication protein	<7.5E-6		E	E [111,112]
lambdap61	<i>P</i>	DNA replication protein	<7.5E-6		E	E [111,112]
lambdap62	<i>ren</i>	protein ren	1.20E-02	7.7E-06	E	NE [113]
lambdap63	<i>ninB</i>	recombination protein NinB	3.00E-05	5.4E-04	E	NE [17,65]
lambdap64	<i>ninC</i>	phosphoadenosine phosphosulfate reductase family protein	clearing on E-1		E	NE [17,65]
	<i>ninD</i>				NT	NE [17,65]
	<i>ninE</i>				NT	NE [17,65]
lambdap67	<i>ninF</i>		4.00E-05	4.0E-06	E	NE [17,65]
lambdap68	<i>ninG</i>	recombination protein NinG	8.0E-06	1.1E-04	E	NE
	<i>ninH</i>				NT	NE [17,65,113]
lambdap70	<i>ninI</i>	serine/threonine phosphatase	4.0E-06	5.8E-06	E	NE [17,65]
lambdap71	<i>Q</i>	antitermination protein	1.6E-05	6.1E-06	E	E [65]
lambdap73	<i>orf-64</i>	hypothetical protein	1.2E-02	9.1E-02	NE	
lambdap74	<i>S</i>	holin/anti-holin	1.0E-05	4.6E-05	E	E [114]
lambdap92	<i>S'</i>	holin/anti-holin	1.0E-05	1.7E-04	E	E [114]
lambdap75	<i>R</i>	endolysin	6.0E-02	5.1E-02	NE	E [115]
lambdap76	<i>Rz</i>	I-spanin	5.0E-04	1.5E-01	E	E [116]
	<i>Rz1</i>				NT	E [116]
lambdap77	<i>bor</i>	serum resistance lipoprotein Bor	7.9E-01	3.0E-01	NE	NE [17]
lambdap78	-	putative envelope protein	1.9E+00	1.3E+00	NE	NE [17]
lambdap79	-	hypothetical protein	3.0E-04	1.1E-04	E	NE [17]
Assay with pQ plasmid						
lambdap62	<i>ren</i>	protein ren	1.20E-02	1.7E+00	NE	NE [113]
lambdap63	<i>ninB</i>	recombination protein NinB	3.00E-01	9.1E-01	NE	NE [17,65]
lambdap64	<i>ninC</i>		1.00E+00	1.5E+00	NE	NE [17,65]
	<i>ninD</i>					NE [17,65]
	<i>ninE</i>					NE [17,65]
lambdap67	<i>ninF</i>		0.03	1.4E+00	NE	NE [17,65]
lambdap68	<i>ninG</i>	recombination protein NinG	0.2	2.1E-01	NE	NE
	<i>ninH</i>					NE [17,65,113]
lambdap70	<i>ninI</i>	serine/threonine phosphatase	1	1.5E+00	NE	NE [17,65]

E, essential; NE, nonessential; NT, not tested.

<https://doi.org/10.1371/journal.pbio.3002416.t001>

Interestingly, the CRISPRi-mediated knockdown of a cluster of delayed early genes (*ren*, *ninB/C/F/G/I*) in the P_R transcriptional unit indicated that all were essential for plaque-formation, contradicting well-established literature [17,63–65]. This “*nin* region” lies between the essential DNA replication genes *O* and *P* and the *Q* gene, encoding the essential late transcription antiterminator. It is known that phages with a deletion of all the *nin* genes retain full plaque-forming ability [63–65]. The simplest interpretation for this discrepancy is that knockdowns in the *nin* region are polar on transcription of gene *Q*, the last gene in the

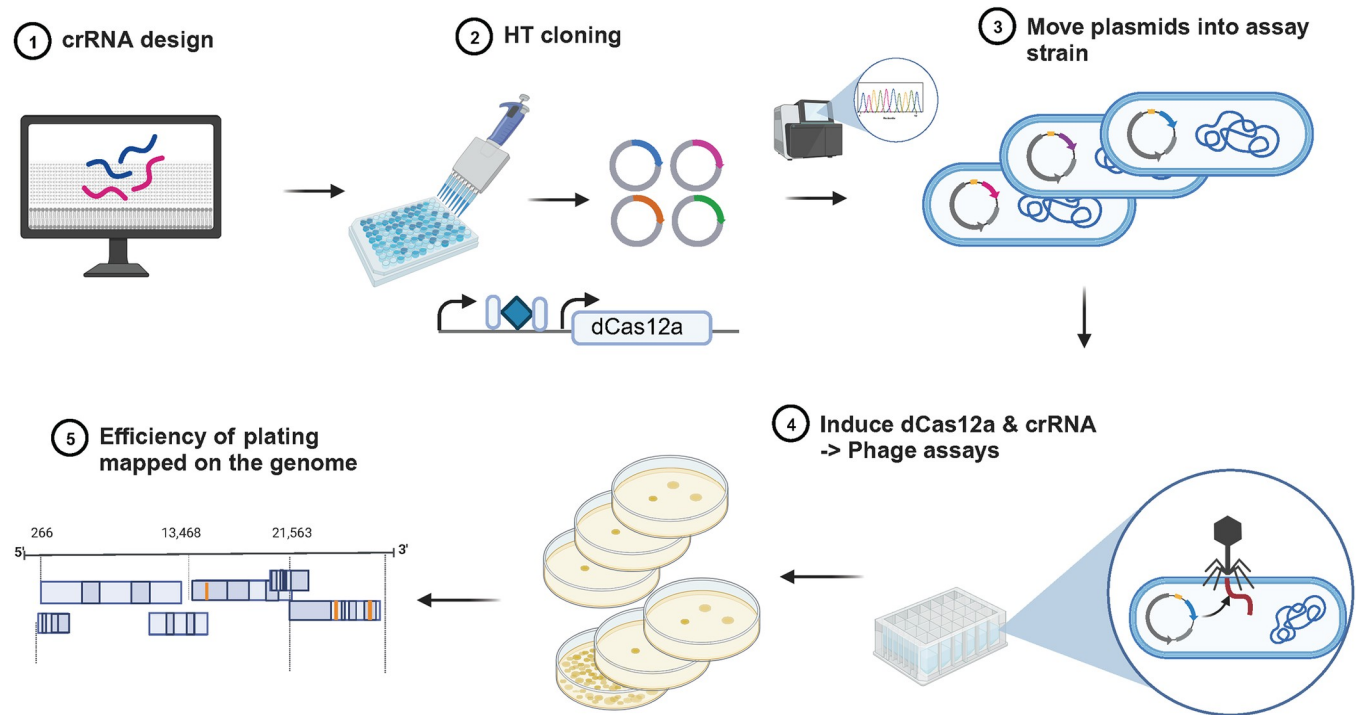


Fig 2. Genome-wide CRISPRi design and assay format. Schematic of steps involved in the arrayed CRISPRi knockdown experiments to assess gene essentiality in phage infectivity cycle. Created with BioRender.com

<https://doi.org/10.1371/journal.pbio.3002416.g002>

transcriptional unit. Polarity has been previously observed for CRISPRi knockdowns in a bacterial context, resulting in false positives in gene function assignments [66–70]. In lambda phage, all genes past *cro* are subject to N-mediated antitermination [17,71], and to our knowledge, CRISPRi knockdowns and polarity effects have not been tested with phage encoded antitermination systems. To determine whether the essential phenotype of the *nin* region genes in our assays is due to polarity on gene Q, we repeated the knockdown assays on an indicator strain that provides Q in *trans* from an inducible plasmid [72]. In these conditions, all 5 genes in the *nin* region targeted by CRISPRi were found to be nonessential, whereas providing Q had no effect on the essentiality of O and P (Figs 3 and S3). These results also conclude that dCas12a-mediated CRISPRi knockdown repression is insensitive to N-mediated antitermination. The Q protein is also an antiterminator and is required for expression of the 27 genes of the late transcript [17,71]. Although most of the genes of this transcript are known to be essential and score that way in our knockdown assays, two of the most promoter-proximal genes score as nonessential, including lambda *orf64* and, to a partial degree, *R*, which shows an intermediate plaque-forming defect. While *R* encodes the endolysin required for lysis, it is known to be produced in great excess, so a significant knockdown might still generate enough bacteriolytic activity to account for the intermediate plaque defect. *Orf64* is indicated to be nonessential [17], but it is unclear why the knockdown is not polar on the many essential genes downstream.

Extending genome-wide CRISPRi assay to coliphage P1

We next extended the genome-wide CRISPRi knockdown assays to assess gene essentiality in coliphage P1. The 93-Kbp genome of P1 is composed of 117 genes, organized into 45 transcriptional units, with 8 involved in the lysis-lysogeny switch and plasmid prophage

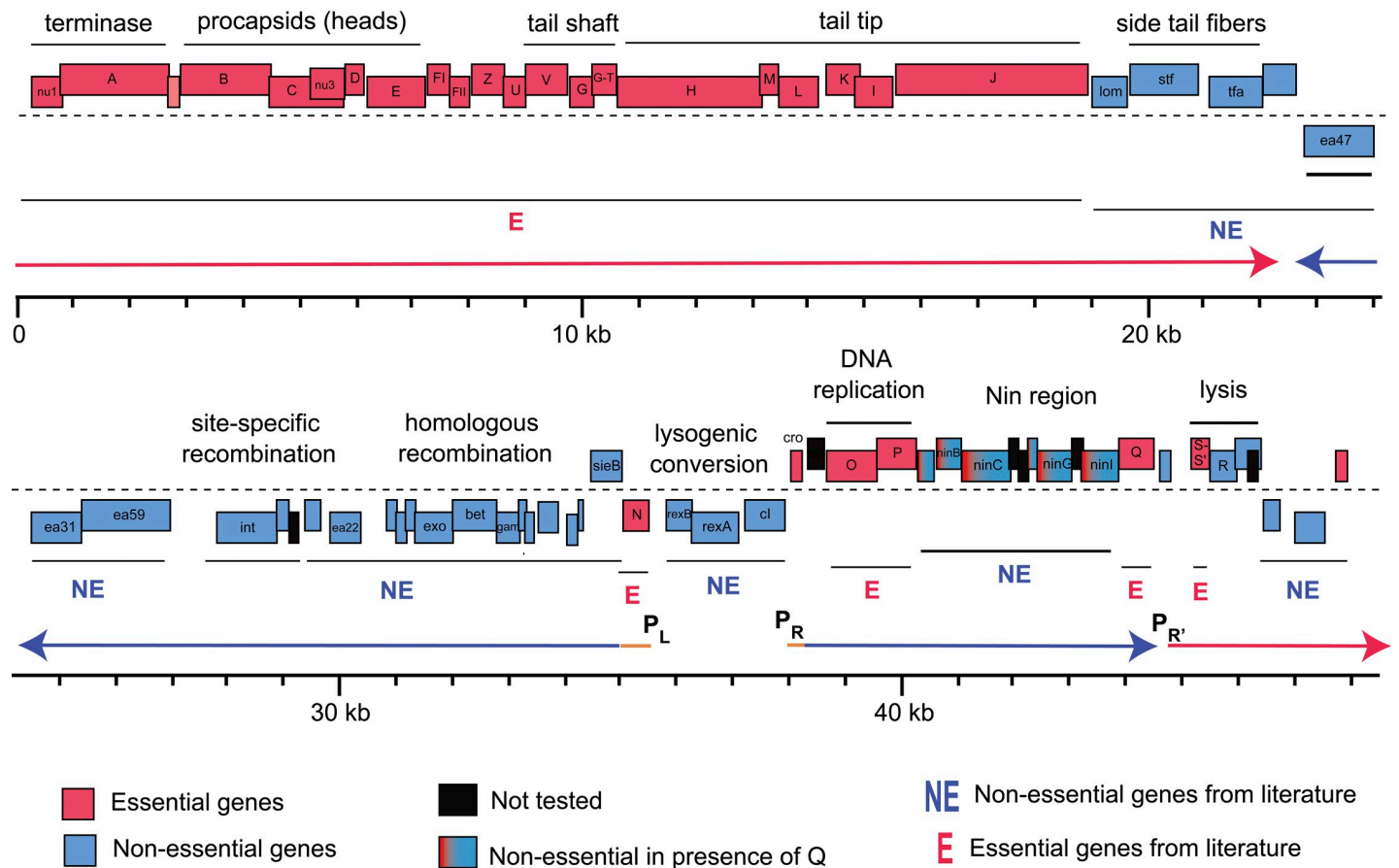


Fig 3. Gene essentiality landscape of phage λ . The genome-wide map of gene essentiality is shown by calculating the EOP as the ratio of plaques appearing on *E. coli* BW25113 lawn expressing crRNA targeting respective lambda phage genes to plaques appearing on BW25113 lawn expressing a nontargeting crRNA. The EOP estimations were done by carrying out biological replicates and depicted the average EOP of every gene on the lambda phage genome map (Methods). Transcripts mentioned in the main text (with promoters) are indicated as thick horizontal arrows: orange, immediate-early transcripts; purple, early transcripts; and red, late transcripts. The underlying data for this figure can be found in [Table 1](#) and [S1 Data](#).

<https://doi.org/10.1371/journal.pbio.3002416.g003>

maintenance, while 37 are involved in lytic development [52]. Despite its paradigm status, a large proportion of gene function assignments still awaits experimental verification [52,73]. Early gene expression and the lytic-lysogenic decision are controlled by the primary phage repressor C1, while Lpa (Late Promoter Activator) positively regulates late transcription. There are 11 late promoters, all of which have a conserved 9 bp inverted repeat that serves as the Lpa-binding site. Compared to lambda, there is no direct experimental evidence of a protein playing a role of antitermination in P1. Nevertheless, there are strong indications that P1 does encode antiterminators [52,74]. Among the 117 genes, 30 have been identified as essential for plaque formation by amber mutant and targeted deletion methods ([Table 2](#) and Notes B in [S1 Text](#)). Experimental evidence for nonessentiality is available for 55 other genes, which makes P1 nearly as good for benchmarking the CRISPR knockdown strategy as lambda.

We designed individual crRNAs targeting 114 out of the 117 genes similar to lambda phage (above); the remaining 3 genes (*upfM*, *pdca*, and *imcA*) were not tested due to lack of PAM sites. Using the same workflow described for lambda, we found 87 genes as nonessential and 27 genes as essential (Figs 4 and S4). Five known essential genes were missed by the knock-down screen: *mat*, *repL*, 25, 26, and *pmgR*. In addition, one gene, *pmgN*, was found to be

Table 2. Gene essentiality mapping of Phage P1 genome.

locus_tag	gene	function [52]	EOP_average	SD	This work	Literature
P1_gp002	<i>cra</i>	cre associated function	6.6E-01	1.3E-01	NE	NE [117,118]
P1_gp003	<i>cre</i>	cyclization recombinase	1.2E+00	8.1E-01	NE	NE [117,118]
P1_gp004	<i>c8</i>	establishment of lysogeny	1.5E+00	3.9E-01	NE	
P1_gp005	<i>ref</i>	recombination enhancement	1.3E+00	3.5E-01	NE	NE [118]
P1_gp006	<i>mat</i>	maturation control	2.8E-01	3.5E-03	NE	E [119]
P1_gp007	<i>res</i>	restriction component	1.2E+00	3.5E-02	NE	NE [120]
P1_gp008	<i>mod</i>	modification component	1.0E+00	3.2E-01	NE	NE [120]
P1_gp009	<i>lxc</i>	modulator of C1 action;	7.0E-01	4.2E-01	NE	NE [121]
P1_gp010	<i>ulx</i>	enhances incorporation of darB	6.4E-01	1.6E-01	NE	NE [122]
P1_gp011	<i>darB</i>	antirestriction	5.8E-01	2.5E-01	NE	NE [122]
P1_gp012	<i>prt</i>	portal	<3.4E-6		E	E [52]
P1_gp013	<i>pro</i>	head processing	<3.4E-6		E	E [52]
P1_gp115	<i>lydE</i>	putative antiholin	9.8E-01	8.8E-01	NE	
P1_gp014	<i>lydD</i>	putative holin	1.1E+00	1.0E-01	NE	
P1_gp015	<i>lyz</i>	lysozyme	5.0E-02	3.5E-03	E	E [123]
P1_gp016	<i>ssb</i>	single stranded DNA binding protein	5.7E-01	2.0E-02	NE	
P1_gp017	<i>isaA</i>	IS1 insertion-associated gene	8.6E-01	4.7E-01	NE	
P1_gp018	<i>insB</i>	IS1 transposition protein	5.1E-01	1.6E-01	NE	
P1_gp019	<i>insA</i>	IS1 transposition protein	1.0E+00	2.2E-01	NE	
P1_gp020	<i>isaB</i>	IS1 insertion-associated gene	1.4E+00	2.2E-01	NE	
P1_gp021	<i>hxr</i>	possible repressor; homolog of Xre	1.6E+00	1.2E+00	NE	NE [122]
P1_gp022	<i>ddrB</i>	antirestriction	8.5E-01	1.3E-01	NE	NE [122]
P1_gp116	<i>iddB</i>	internal to ddrB	5.4E-01	2.6E-01	NE	NE [122]
P1_gp023	<i>ddrA</i>	antirestriction	9.8E-01	3.1E-01	NE	NE [122]
P1_gp024	<i>darA</i>	antirestriction	6.5E-01	2.9E-01	NE	NE [122]
P1_gp025	<i>hdf</i>	antirestriction	1.2E+00	8.4E-01	NE	NE [122]
P1_gp026	<i>lydB</i>	lysis determinant; prevents premature lysis	2.3E-02	2.6E-02	E	NE [123,124]
P1_gp027	<i>lydA</i>	holin	1.2E-01	2.4E-03	NE	NE [123,124]
P1_gp028	<i>lydC</i>	holin	1.1E+00	1.2E-01	NE	
P1_gp029	<i>cin</i>	site-specific recombinase	1.4E+00	9.5E-01	NE	NE [125]
P1_gp001	<i>Sv prime</i>	C-terminal moiety of tail fiber gpS	5.3E-01	3.2E-01	NE	NE [126]
P1_gp030	<i>U prime</i>	structural protein gpU prime of tail fiber	8.6E-01	8.0E-01	NE	NE [126]
P1_gp031	<i>U</i>	tail fiber structure or assembly	<5.2E-5		E	
P1_gp032	<i>S</i>	tail fiber structure or assembly	<5.2E-5		E	
P1_gp033	<i>R</i>	tail fiber structure or assembly	<5.2E-5		E	E [127]
P1_gp034	<i>16</i>	baseplate or tail tube	<5.2E-5		E	E [128]
P1_gp035	<i>bp1A</i>	putative baseplate structure, may correspond to gene 3	<2.9E-5		E	
P1_gp036	<i>pmgA</i>	Putative morphogenetic function	<2.9E-5		E	E [73]
P1_gp037	<i>sit</i>	putative tape measure protein	<2.9E-5		E	
P1_gp038	<i>pmgB</i>	Putative morphogenetic function	<2.9E-5		E	E [73]
P1_gp039	<i>tub</i>	tail tube	<2.9E-5		E	
P1_gp040	<i>pmgC</i>	Putative morphogenetic function	<2.9E-5		E	E [73]
P1_gp041	<i>simC</i>	superimmunity	1.7E+00	6.9E-01	NE	NE [129]
P1_gp042	<i>simB</i>	superimmunity	3.8E+00	8.4E-01	NE	NE [129]
P1_gp043	<i>simA</i>	superimmunity	9.0E-01	4.9E-01	NE	NE [129]

(Continued)

Table 2. (Continued)

locus_tag	gene	function [52]	EOP_average	SD	This work	Literature
P1_gp044	<i>c4 RNA</i>	acts on <i>icd</i> and <i>ant</i> mRNA	8.3E-01	9.4E-01	NE	
P1_gp045	<i>icd</i>	reversible inhibition of cell division	6.0E-01	2.2E-01	NE	NE [130]
P1_gp046	<i>ant1</i>	antagonizes C1 repression1	2.0E+00	1.1E+00	NE	NE [131]
P1_gp047	<i>ant2</i>	product antagonizes C1	2.3E+00	1.8E+00	NE	NE [131]
P1_gp048	<i>ask</i>	regulatory region of <i>kilA</i> gene;	1.2E+00	4.9E-01	NE	
P1_gp049	<i>kilA</i>	product can kill host	8.6E-01	8.0E-01	NE	NE [131]
P1_gp050	<i>repL</i>	initiates replication at <i>oriL</i>	7.1E-01	3.0E-01	NE	NE [131]
P1_gp051	<i>rlfA</i>	possibly associated with lytic replication	1.3E+00	6.1E-02	NE	
P1_gp052	<i>rlfB</i>	possibly associated with lytic replication	8.8E-01	3.0E-02	NE	
P1_gp053	<i>pmgF</i>	putative morphogenetic function	1.2E+00	1.0E-02	NE	NE [73]
P1_gp054	<i>bplB</i>	baseplate structure	<1.2E-7		E	
P1_gp055	<i>pmgG</i>	putative morphogenetic function	<1.2E-7		E	E [73]
P1_gp056	21	baseplate or tail tube	<1.2E-7		E	* [128]
P1_gp057	22	tail sheath	<1.2E-7		E	* [128]
P1_gp058	23	Major head protein	<1.2E-7		E	* [128]
P1_gp059	<i>parB</i>	active partitioning of P1 plasmid during cell division	1.3E+00	7.6E-01	NE	
P1_gp060	<i>parA</i>	active partitioning of P1 plasmid during cell division	1.6E+00	1.5E+00	NE	
P1_gp061	<i>repA</i>	initiates replication from <i>oriR</i> ; plasmid replication	9.5E-01	6.4E-02	NE	
P1_gp062	<i>upfA</i>		1.2E+00	8.9E-01	NE	NE [73]
P1_gp063	<i>mlp</i>	membrane lipoprotein precursor	2.4E-01	1.9E-01	NE	
P1_gp064	<i>ppfA</i>	possible periplasmic function	1.3E+00	1.2E+00	NE	
P1_gp065	<i>upfB</i>		1.3E+00	1.0E+00	NE	NE [73]
P1_gp066	<i>upfC</i>		1.1E+00	6.8E-01	NE	NE [73]
P1_gp067	<i>uhr</i>		8.6E-01	1.9E-01	NE	NE [73]
P1_gp068	<i>hrdC</i>	hpothetical recombination associated protein of RdgC family	8.7E-01	4.6E-01	NE	
P1_gp069	<i>dmt-B</i>	DNA methyltransferases; methylsates A at GATC	1.4E+00	1.2E+00	NE	NE [132]
P1_gp070	<i>dmt-A</i>		1.4E+00	7.6E-03	NE	
P1_gt071	<i>trnT</i>		9.2E-01	4.0E-01	NE	
P1_gp072	<i>plp</i>	putative lipoprotein	1.6E+00	8.2E-01	NE	
P1_gp073	<i>upl</i>		1.9E+00	5.9E-01	NE	NE [73]
P1_gp074	<i>tciA</i>	tellurite or colicin resistance or inhibition of cell division	6.5E-01	6.5E-02	NE	
P1_gp075	<i>tciB</i>	tellurite or colicin resistance or inhibition of cell division	9.9E-01	1.0E-01	NE	
P1_gp076	<i>tciC</i>	tellurite or colicin resistance or inhibition of cell division	1.3E+00	4.4E-01	NE	
P1_gt117	<i>trnI</i>		1.4E+00	7.9E-01	NE	
P1_gp077	<i>ban</i>	<i>dnaB</i> homolog	1.2E+00	4.8E-01	NE	NE [133]
P1_gp078	<i>dbn</i>	downstream of <i>ban</i>	1.3E+00	1.3E-01	NE	NE [73]
P1_gp079	5	baseplate	<2.1E-6		E	* [128]
P1_gp080	6	tail length	8.3E-03	1.3E-03	E	* [128]
P1_gp081	24	baseplate or tail stability	4.9E-03	5.0E-03	E	* [128]
P1_gp082	7	tail stability	<8.2E-6		E	* [128]

(Continued)

Table 2. (Continued)

locus_tag	gene	function [52]	EOP_average	SD	This work	Literature
P1_gp083	25	tail stability	1.1E-01	6.6E-02	NE	* [128]
P1_gp084	26	baseplate;	1.2E-01	1.5E-01	NE	* [128]
P1_gp085	<i>pmgL</i>	putative morphogenetic function	1.3E+00	9.4E-01	NE	NE [73]
P1_gp086	<i>pmgM</i>	putative morphogenetic function	3.8E-01	2.1E-01	NE	NE [73]
P1_gp087	<i>pmgN</i>	putative morphogenetic function	1.4E-02	1.5E-03	E	NE [73]
P1_gp088	<i>pmgO</i>	putative morphogenetic function	1.1E+00	8.7E-01	NE	NE [73]
P1_gp089	<i>pmgP</i>	putative morphogenetic function	7.2E-01	7.3E-02	NE	NE [73]
P1_gp090	<i>ppp</i>	protein phosphatase	1.2E+00	8.0E-02	NE	NE [73]
P1_gp091	<i>pmgQ</i>	putative morphogenetic function	1.4E+00	7.5E-01	NE	NE [73]
P1_gp092	<i>pmgR</i>	putative morphogenetic function	9.4E-01	3.0E-01	NE	E [73]
P1_gp093	<i>pmgS</i>	putative morphogenetic function	1.2E+00	3.2E-01	NE	NE [73]
P1_gp094	<i>pap</i>	acid phosphatase	7.7E-01	2.3E-01	NE	NE [73]
P1_gp095	<i>pmgT</i>	putative morphogenetic function	9.8E-01	9.7E-01	NE	NE [73]
P1_gp096	<i>pmgU</i>	putative morphogenetic function	2.1E-01	6.4E-02	NE	NE [73]
P1_gp097	<i>pmgV</i>	putative morphogenetic function	1.9E+00	2.0E+00	NE	NE [73]
P1_gp098	<i>upfM</i>	unknown protein function			NT	NE [73]
P1_gp099	<i>upfN</i>	unknown protein function	8.3E-01	2.4E-01	NE	NE [73]
P1_gp100	<i>upfO</i>	unknown protein function	9.5E-01	6.4E-01	NE	NE [73]
P1_gp101	<i>hot</i>	DNA replication	1.2E+00	1.6E+00	NE	
P1_gp102	<i>lxr</i>	LexA-regulated functions	7.9E-01	7.7E-01	NE	
P1_gp103	<i>humD</i>	DNA repair	5.4E-01	3.3E-01	NE	
P1_gp104	<i>phd</i>	anti-toxin of P1 toxin-antitoxin system	5.5E-01	7.1E-02	NE	
P1_gp105	<i>doc</i>	toxin of P1 toxin-antitoxin system	3.6E-01	1.2E-02	NE	
P1_gp106	<i>pdca</i>	unknown protein function			NT	NE [73]
P1_gp107	<i>pdcb</i>	unknown function	6.8E-01	2.6E-01	NE	NE [73]
P1_gp108	<i>lpa</i>	late promoter activator	<1.2E-7		E	* [134]
P1_gp109	<i>pacA</i>	DNA packaging	<1.2E-7		E	* [135]
P1_gp110	<i>pacB</i>	DNA packaging	<1.2E-7		E	* [135]
P1_gp111	<i>c1</i>	lytic repressor	1.4E+00	1.3E+00	NE	
P1_gp112	<i>coi</i>	C1 inactivator	7.4E-01	8.4E-01	NE	NE [136]
P1_gp113	<i>imcB</i>	immunity function	8.2E-01	7.3E-01	NE	
P1_gp114	<i>imcA</i>	immunity function			NT	

E, essential; NE, nonessential; NT, not tested.

* amber mutant reported

<https://doi.org/10.1371/journal.pbio.3002416.t002>

essential, in contradiction with the recent deletion analysis survey [73]. From the perspective of identifying nonessential genes, 54 of the 55 genes for which there was some evidence of non-essential character were confirmed by the knockdown. In addition, the knockdown approach demonstrates nonessentiality for a further 33 genes. Taken together, 4 large segments comprising nearly 60 kb of the P1 genome are occupied by genes dispensable for lytic growth and thus available for specific engineering (Table 2).

Downstream application of gene essentiality mapping

To demonstrate one downstream application of the knockdown approach to gene essentiality mapping, we sought to insert a unique DNA tag into both λ and P1 at a gene locus that we

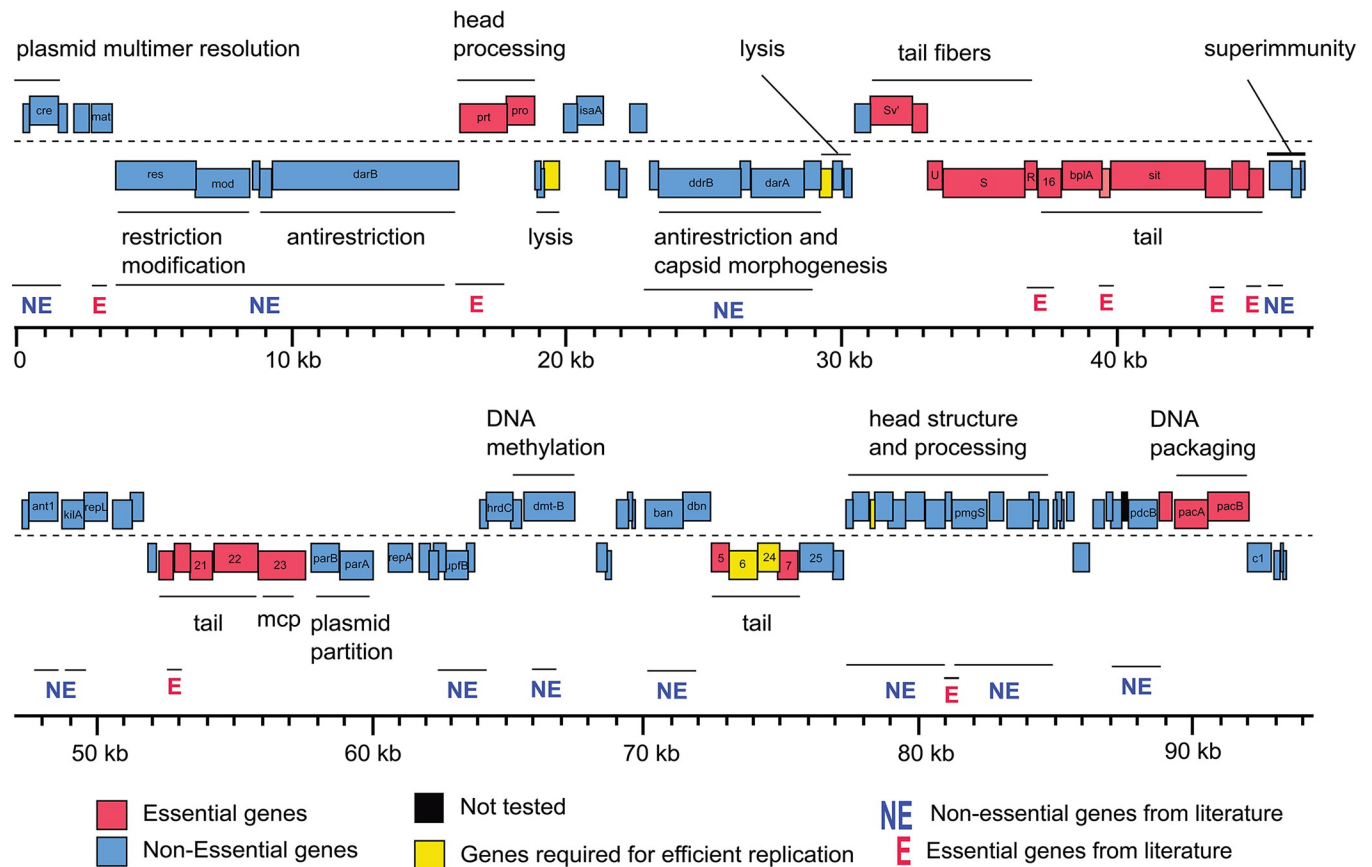


Fig 4. Gene essentiality landscape of phage P1. The genome-wide map of gene essentiality is shown by calculating the EOP as the ratio of plaques appearing on *E. coli* BW25113 lawn expressing crRNA targeting respective P1 phage genes to plaques appearing on BW25113 lawn expressing a nontargeting crRNA. The EOP estimations were done by carrying out biological replicates and depicted the average EOP of every gene on the P1 phage genome map (Methods). The underlying data for this figure can be found in Table 2 and S1 Data.

<https://doi.org/10.1371/journal.pbio.3002416.g004>

found to be dispensable. As DNA barcodes are heritable, they can be used for rapid identification of different phage samples by standardizing the workflow, assuming their insertion does not impact phage fitness. Such unique barcoding of different phages could enable quantitative tracking and measure of individual phage fitness in multiphage formulations in different applications.

As a proof of concept, we inserted a unique DNA barcode in genes *res* and *red*, of P1 and lambda, respectively. We used a homologous recombination approach followed by nuclease active Cas12a-based counter selection for barcoded phages in a 2-step process (Methods). Successful DNA barcode insertions into phage genomes were then confirmed by Sanger sequencing of the insertion locus. With these 2 *bc* (barcoded) constructs, we tested whether we could quantify different phage combinations. To do this, we mixed phage P1-*bc* and λ -*bc* in different ratios, incubated at room temperature for 30 minutes, and subjected them to Barseq PCR sequencing [75,76]. Our Barseq quantification method not only successfully quantified different ratios of barcoded phage P1 and lambda but also captured the differences in plaque-forming units/ml of individual phages to barcode abundance (Fig 5).

Discussion

CRISPR-based technologies have revolutionized the functional genomics field [34]. CRISPRi, in particular, has emerged as a major technology for genome-wide mapping of essential and

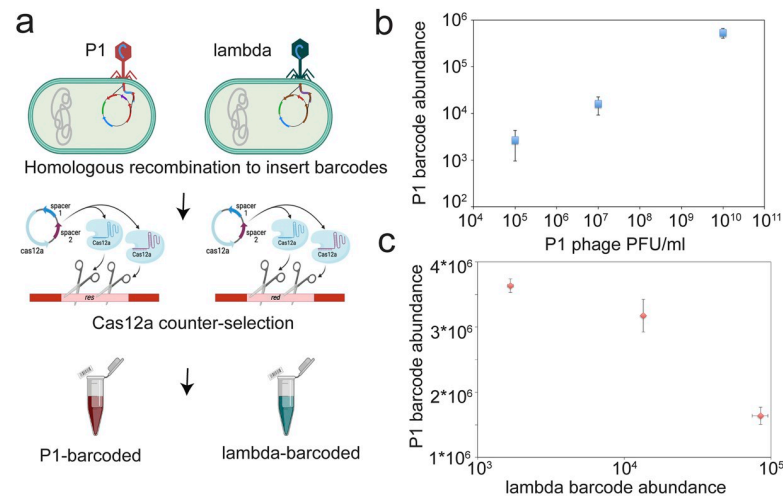


Fig 5. Insertion and quantification of random DNA barcodes on a nonessential genomic location of lambda and P1vir phage. (a) Schematic of phage engineering approach: Homologous recombination method was used to engineer phages with random barcodes at a nonessential genomic loci, and nuclease active Cas12a-based counterselection was used to enrich engineered phages. Schematic is shown for barcode insertion and counterselection for lambda phage at the *red* locus and P1 phage at *res* locus. Created with [BioRender.com](https://www.biorender.com/). (b) Barcode abundance of P1 phage against its PFU/ml estimations in triplicates. (c) Barcode abundance for both barcoded lambda and P1 phages, when mixed at different ratios. Estimations done in triplicates in a pool (Methods). The underlying data for this figure can be found in [S1 Data](#).

<https://doi.org/10.1371/journal.pbio.3002416.g005>

nonessential genes in bacteria [34,35]. Here, we assessed the feasibility of using dCas12a system for performing a genome-wide survey of 2 paradigm phages, lambda and P1, using crRNAs designed to achieve gene-specific “knockdown.” Results from our arrayed CRISPRi assays are consistent with known assignments of gene essentiality in both phages, provide novel insights, and present a genome-wide landscape of gene essentiality for phage P1 for the first time, to the best of our knowledge (Tables 1 and 2 and Figs 3 and 4). Lambda and P1 phages have quite distinct transcriptional organization, making CRISPRi differentially suited for probing stretches of nonessential genes in these phages (below). With an organized map of gene essentiality in hand, it is now possible to identify locations in these phage genomes wherein insertion of an exogenous “payload” are less likely to disrupt critical function, as well as longer regions that can be deleted or replaced with custom DNA. As a proof of principle, we demonstrate this by inserting a DNA barcode into the lambda and P1 genome at an inessential loci that provides the ability to track and quantify distinct phages in a mixed phage formulation. Finally, this study uncovers the polar effect of CRISPRi in phages. We recommend using CRISPRi for mapping nonessential regions while caution towards interpreting essential gene assignments when applied to less studied phages where transcripts have not yet been mapped. We discuss these insights below.

Overall, the genome-wide CRISPRi assay results demonstrated dCas12a was effective; that is, nearly every nonessential lambda gene knockdown was scored correctly, and essential lambda genes were scored as essential, based on reduction of plating efficiency by 3 powers of 10 or more in the presence of dCas12a and the cognate crRNA (Fig 3 and Table 1). However, a cluster of delayed early genes in the *nin* region of the P_R transcript of lambda were scored as essential despite unambiguous evidence that this entire region can be deleted without impairing the plaque-forming ability of the phage [63–65]. Because of its DNA-binding function, the bound dCas12a/crRNA complex is necessarily a roadblock that would be polar on all

downstream genes, as confirmed experimentally for the knockdowns of *lacZ* in the *lacZYA* operon of *E. coli* [38]. The reason for this polarity is because this cluster of nonessential *nin* genes is upstream of gene Q, which encodes the late-gene activator required for late-gene expression. Thus, roadblocks in the *nin* genes should be polar on gene Q. Accordingly, when we supplied Q *in trans*, the *nin* genes all scored properly as nonessential (Fig 3). Unfortunately, the same rationale applies to the other genes served by P_R (Fig 3). Thus, knockdowns in *cro*, *O*, and *P* are also polar on Q. With Q added in *trans*, all 3 upstream genes read out as essential but only the gene *P* result is confirming, since the *cro* and *O* knockdowns should be polar on essential gene *P*. The situation is better for the P_L transcriptional unit because the only essential gene is the first one, *N*. Thus, for P_L, all 19 genes that were tested are scored correctly, as nonessential.

Similar challenges for CRISPRi essentiality determination are noted for the late genes, expressed from P_R in a 27-kb mRNA (Fig 3). Twenty-one genes from *nu1* through *J* read out correctly as essential, but since the first 20 knockdowns should be polar on J, nothing can be concluded for their essentiality based on CRISPRi results. Moreover, the results for the upstream genes *orf64* and *R* are confounding. From the same perspective as used on the P_R transcript, knockdown roadblocks in all the upstream genes in this transcriptional unit should be read out as essential. This was observed for gene *p79* (which is nonessential, but essential in our assay), but it was not observed for the knockdowns of *orf64* and *R*. In CRISPRi studies on bacterial genomes [66–70,77], similar polarity issues have been noted, and contradictions have been explained by invoking the presence of cryptic promoters downstream of the roadblock site [69]. For a phage like lambda, where transcriptional organization has been unambiguously established by rigorous genetics and molecular approaches (though new technologies are providing new information [78]), these arguments may not hold. The simplest possibility is that there are large variations in the effectiveness of each roadblock [79], despite the perfect match of 28 nucleotides in each crRNA and, in each case, a TTTV PAM sequence. Hence, in the absence of data assessing the level of readthrough in the *orf64* and *R* roadblocks, useful interpretation of the P_R results is not practical. An intriguing possibility is that Q-mediated antitermination may play a role in readthrough of these CRISPRi roadblocks. It is widely unappreciated that for all the well-studied phages, late gene expression is always under positive control, either by an antiterminator like lambda Q and the P_R promoter or by a transcription factor like Lpa and the 11 late promoters of P1 [17,52]. It would be interesting to determine quantitatively how such positive control factors affect the efficacy of Cas12a in CRISPR defense and dCas12a in roadblock knockdowns, with an eye towards possible evolutionary interactions. In any case, the results from knockdowns in the 3 major transcripts of lambda show that only *N*, *P*, *Q*, and *J* can be confidently established as essential genes. Thus, as noted earlier [66], the nature of CRISPRi roadblock polarity means that essentiality can only be assigned for the last required gene on a transcript. The 2 major lessons from our work on lambda are, first, CRISPRi polarity could assign false positive gene essentiality and therefore recommend caution when applied to less studied phages; and, second, CRISPRi based on DNA roadblocks is of limited utility for analysis of phages that, like lambda, feature long polycistronic transcriptional units. However, for the more utilitarian goal of identifying significant swaths of the phage genome that could be considered “nonessential” and thus available for engineering, this approach still has high value. All of the 14-kb P_L transcript beyond *N*, comprising 15 genes, score unambiguously as nonessential.

Among phage genomes, lambda is arguably the best characterized transcriptional system because of its simplicity, with only 3 promoters involved in lytic development. P1 stands in stark contrast, with at least 45 transcriptional units, including 15 monocistronic units, and several genes served by both early and late promoters. In general, similar results were obtained

from the genome-wide knockdown approach as with lambda (Fig 4 and Table 2). Of the 31 genes assigned essential character in the extensive P1 literature, all but 5 were detected by the knockdown screen. However, consideration of the transcript structures and gene positions reveals that of the 26 genes that read out as essential, 18 are located upstream of a gene known to be essential, and, thus, the knockdown readout is uninformative. Moreover, as in the case for the promoter-proximal genes in the lambda late transcriptional unit, P1 has a confounding transcript. Genes 25 and 26, which were discovered as amber mutants and thus must be considered as known essentials, both score as nonessential genes in our assays. This constitutes a double contradiction, not only in the failure to detect essential character but also not exhibiting polarity on the cluster of genes downstream (genes 7, 24, 6, and 5) that correctly read out as required cistrons. The simplest notion is that for some reason, neither the 25 nor 26 roadblocks are effective. Quantitative assessment of roadblock readthrough is beyond the scope of this initial validation screen, but it would be useful to determine the level of blockage and readthrough throughout the lambda and P1 libraries (as recently reported for *E. coli* [79]). This is especially true since the 2 confounding cases (genes *orf64* and *R* in lambda; genes 25 and 26 in P1) are at the 5' end of a polycistronic transcriptional unit. Unlike other CRISPRi systems, the dCas12a roadblocks are reported to be independent of promoter-proximity, but that lesson has only been addressed within the *lacZYA* cistron [38], and not for very long transcripts or for transcriptional units under the positive control of an antiterminator.

Because of tightly overlapped and transcriptionally linked genetic elements in phages, such polarity effects may be difficult to overcome using CRISPRi. The catalytically inactive version of recently reported RNA-targeting Cas13 system might solve some of the polarity effect issues associated with DNA-targeting Cas systems by modulating translation of single genes encoded within operons [29,31]. In addition, the absence of PAM requirements for Cas13 targeting and its broad-spectrum phage targeting capability may enable designing multiple crRNA targeting the same genomic locus, to quickly and comprehensively map gene essentiality landscape in diverse phages [29]. Nevertheless, in contrast to classical genetic methods such as recombining, that require cumbersome cloning of long homology arm pairs followed by plaque screening to identify edited phages that exist at low abundance relative to wild-type, arrayed CRISPRi assay as presented here offers a simpler and economical approach that only requires cloning a set of short crRNA sequences. By using pooled crRNAs, it may be possible to extend the CRISPRi technology to carry out pooled fitness assays and identify phage genes important in the phage life cycle in a single rapid assay. While this manuscript was under review, successful implementation of dCas13 based genome-wide pooled CRISPRi screen was reported for diverse phages [80] and point to a rich future of diverse functional genomics tools to study phage biology.

Even though the gene essentiality mapping results are dependent on the experimental settings and conditions used in the assay systems, they do open up interesting questions and avenues to assess the role of nonessential and accessory genes in phage development and infection pathways [15,17,18]. By adopting high-throughput CRISPRi assays to map phage gene essentiality in different conditions [81], it may be possible to study the role of such conditional gene essentiality in phage infection. Furthermore, the simple multiplexability of dCas12a crRNAs (for example, dual crRNAs targeting 2 genes) could enable rapid, systematic investigation of synthetic lethal phage gene pairs. Extending such studies to non-model, non-dsDNA phages may further provide us with deeper information needed to study genomic architecture and phage engineering applications. Considering that the different CRISPR-based tools have been successfully applied to multitudes of microbial species [34,82] and have been used to engineer diverse phages, we expect CRISPRi technology to serve as a powerful approach to rapidly identify nonessential and accessory genes and pathways in phage infection cycles.

Methods and materials

Bacterial strains and phages

The bacterial strains and phages used in this study are listed in [S1 Table](#). The oligonucleotides used in this study are listed in [S2 Table](#). All enzymes were obtained from New England Biolabs (NEB), and oligonucleotides were received from Integrated DNA Technologies (IDT). Unless noted, all strains were grown in LB supplemented with appropriate antibiotics at 37°C in the Multitron shaker. All bacterial strains were stored at -80°C for long-term storage in 15% sterile glycerol (Sigma). The genotype of *E. coli* strains used in the assays include BW25113 (K-12 *lacI+rrnBT14 Δ(araB-D)567 Δ(rhaD-B)568 ΔlacZ4787(::rrnB-3) hsdR514 rph-1*); MG1655 (F-lambda- *ilvG- rfb-50 rph-1*) and *E. coli* C3000 (ATCC15597).

E. coli strains were cultured in LB (Lennox) [10 g/L Tryptone, 5 g/L NaCl, 5 g/L yeast extract] or LB agar [LB (Lennox) with 1.5% Bacto agar] at 37°C. *E. coli* strains transformed with plasmids were selected in the presence of 100 µg/mL ampicillin (LB Amp) or 30 µg/mL chloramphenicol (LB cam). Phages were plated using 0.5% top agar [10 g/L Tryptone, 10 g/L NaCl, 5 g/L Bacto agar]. Before plating, 5 mM CaCl₂ and 5 mM MgSO₄ were added to top agar aliquots.

The phages (lytic phages, λcI857 and P1vir) used in this study were prepared by the confluent plate lysis method using LB bottom plates and 0.5% top agar [83]. Phages were harvested in SM buffer (Teknova), filter sterilized, and stored at 4°C. Plaque assays were performed using spot titration method [83].

Design and construction of spacer duplex

Cas12a recognizes TTTV as the PAM site [53]. For each target gene, PAM sites for Cas12a were identified to serve as toe-holds for the crRNAs. As any genes could have an alternative start site, the PAM sites nearby the annotated start codon of the gene were avoided. To avoid end effects, and based on prior experience in bacterial CRISPRi [70], PAM sites were prioritized if they occurred after 20% of the gene length (so that the dCas12a complex would bind to approximately on the 1/5th position of the gene). The 28-bp nucleotide sequences immediately downstream of the PAM site in the coding strand were selected as the protospacer region. The forward oligo was designed by adding sequences “AGAT” to the 5′ region of the protospacer sequence and sequence “G” to the 3′ region of the protospacer sequence to make the ends of oligos Golden Gate cloning compatible. The reverse oligo was designed by reverse complementing the protospacer sequence from the coding strand and adding sequences “GAAAC” to the 5′ end. Custom python scripts (<https://github.com/NickNolan/phage-crispri>) were designed for identifying the protospacer regions and respective oligonucleotides.

We processed oligonucleotides by carrying out 5′ phosphorylation and annealing of complementary oligonucleotides in a single tube reaction. The published sequences for phages P1 (NCBI Reference Sequence: NC_005856.1) and λ (NCBI Reference Sequence: NC_001416.1) were used as reference sequences to generate oligos. Each 5 µL reaction comprised 0.5 µL each of the forward and reverse oligonucleotide pair (100 µM stock), 0.5 µL of 10× T4 DNA Ligase Reaction Buffer (NEB), 0.5 µL T4 Polynucleotide Kinase (NEB). The reaction was carried out in a thermocycler as follows: 37°C for 30 minutes, 95°C for 5 minutes, followed by gradient decrease of temperature from 95°C to 25°C (0.5°C every 6 seconds for 140 cycles). To make a working stock of the spacer duplex, the reaction mix was diluted to a final volume of 100 µL by adding milliQ water.

Plasmid construction

The plasmid collection used in this study is listed in [S3 Table](#). All plasmid manipulations were performed using standard molecular biology techniques. The plasmid system encoding

nuclease active LbCas12a has been described previously [53]. In brief, LbCas12a is cloned under aTc-inducible Tet promoter, whereas the CRISPR arrays are constitutively transcribed from a strong, synthetic promoter proD [53]. For CRISPRi, catalytically deactivated LbCas12a (dLbCas12a) lacking endonuclease activity was generated by the mutating nuclease domain of LbCas12a. For each CRISPRi plasmid, a spacer targeting a specific phage gene was cloned into the CRISPR array using Golden Gate assembly [84]. Each 5 μ L of the reaction contained 0.5 μ L of ATP (NEB), 0.5 μ L DTT (1 mM final concentration), 0.5 μ L 10 \times CutSmart Buffer (NEB), 0.375 μ L BbsI (NEB), 0.125 μ L T4 Ligase (NEB), 20 fmol CRISPRi plasmid, and 100 fmol spacer duplex (0.2 μ L of the working stock of the spacer duplex). The reaction was cycled between 37°C and 20°C for 5 minutes each at each temperature for 30 cycles and heat inactivated at 80°C for 20 minutes. This same method was followed to clone the spacer duplex into the plasmid encoding nuclease active version of LbCas12a.

For inserting a random DNA barcode into a nonessential region of phage (*res* and *cra-darB* region in P1 phage while *red* gene in lambda; S3 Table), a recombination template was constructed on pBAD24 vector backbone [85]. A synthetic dsDNA was obtained from IDT as a gBlock gene fragment that comprised 2 homology arms, each of 100-bp homology to the non-essential region of the phage genome [86]. In between the two 100-bp homology arms, a random 20-bp DNA barcode flanked by 2 primer-binding regions was inserted so that the barcoded phage genome could be assayed by high-throughput DNA barcode sequencing (BarSeq) technology [75]. The gBlock fragment was PCR amplified and cloned into a PCR-amplified pBAD24 backbone using Gibson assembly [87].

The Golden Gate or Gibson assembly mixture was transformed into competent *E. coli* 5-alpha cells (NEB) following manufacturer's recommendations and selected by plating on LB in the presence of appropriate antibiotics. Successful insertion into the plasmid backbone was verified by Sanger sequencing (UC Berkeley DNA Sequencing Facility or Elim Biopharmaceuticals). These pBAD24-derived plasmids would serve as recombination templates.

CRISPRi assays for mapping phage gene essentiality

For CRISPRi knockdown assays, each variant of the CRISPRi plasmid was transformed into *E. coli* str. BW25113 using standard method [88] and selected on independent LB cam plates. An overnight culture of the transformed strain was used to prepare a lawn on LB cam supplemented with 2 nM or 4 nM aTc for induction of the dCas12a. Phages were serially diluted 10-fold, and 2 μ L of each dilution was plated on a lawn of bacterial host. The number of plaques was quantified after overnight incubation at 37°C. The EOP was calculated as the ratio of plaques appearing on BW25113 lawn expressing crRNA targeting respective phage genes to plaques appearing on BW25113 lawn expressing nontargeting crRNA. The nontargeting crRNA targets P1 phage gene 23 in lambda CRISPRi assays while it targets lambda phage gene *E* in P1 CRISPRi assays. The complete compendium of EOP for each CRISPRi knockdown assay for lambda and phage P1 is listed in Tables 1 and 2, respectively.

To assess the essentiality of the Nin region in λ cI857, we transformed all *nin* targeting CRISPRi plasmids into *E. coli* str. BW25113, carrying a pQ plasmid system [72], and carried out CRISPRi knockdown assays as described above (S3 Fig). The plasmid pQ, a low-copy plasmid carrying Q, encodes the λ late gene activator under control of a *lac/ara* hybrid promoter, which is inducible with IPTG and arabinose.

To determine the conditional essentiality of *ral*, we transformed the *ral* targeting CRISPRi plasmid into *E. coli* MG1655 and C3000 strains and carried out CRISPRi knockdown assays in the presence of lambda phage as described above. Both *E. coli* MG1655 and C3000 strains encode an active type I restriction system. The plaque-forming efficiency was compared

between *E. coli* lawn expressing crRNA targeting *ral* and *P* genes and with plaques appearing on *E. coli* lawn expressing nontargeting crRNA.

Engineering DNA barcoded phages

For inserting the DNA barcode into the phage genome, pBAD24-derived plasmid (S3 Table) was transformed into *E. coli* str. BW25113 using a 1-step transformation method [88]. Phage stock was appropriately diluted and plated on the lawn of the transformed BW25113 host using full-plate titration method [83]. Individual plaques were picked from the lawn, and the insertion of the DNA barcode was verified by PCR amplifying the junction and Sanger sequencing. The phages obtained from each plaque had a mixed population of unmodified and recombinant phage. This mixed population of phages were further enriched by confluent lysis plating method, and the wt phage in each plaque was counterselected by plating the mixture phage on the lawn of BW25113 host expressing nuclease active Cas12a target the nonessential region of the phage [89].

Barseq assays using DNA barcoded phages

To demonstrate the utility of barcoded phages, we mixed uniquely barcoded P1 and lambda phage lysates in different ratios, in triplicates. To benchmark the barcoded phage quantification with a set of internal controls, we spiked 4 uniquely barcoded *E. coli* genome preparation into each of the Barseq samples. For performing Barseq PCR reactions, we used phage lysates as templates mixed with *E. coli* genome preparations. BarSeq PCR in a 50- μ l total volume consisted of 20 μ mol of each primer. We used an equimolar mixture of BarSeq_P2 primers along with new Barseq3_P1 primers as detailed earlier [75,90]. Briefly, the BarSeq_P2 primer contains the tag that is used for demultiplexing by Illumina software, and the new Barseq3_P1 primer contains an additional sequence to verify that it came from the expected sample (as described earlier) [90]. All experiments were done on the same day and sequenced on the same lane. Equal volumes (5 μ l) of the individual BarSeq PCRs were pooled, and 50 μ l of the pooled PCR product was purified with the DNA Clean and Concentrator kit (Zymo Research). The final BarSeq library was eluted in 40 μ l water. The BarSeq libraries were sequenced on Illumina HiSeq4000 instrument with 50 SE runs. We used in-house Barseq PCR processing code for estimating DNA barcodes in samples [75].

Supporting information

S1 Fig. Lambda phage genome CRISPRi oligo designs. Blue represents genes, red represents primers, and black is the full genome. Outside is on the positive strand, where inside is negative.

(TIF)

S2 Fig. Conditional essentiality of lambda *ral* in presence of an active type I restriction-modification system encoded by *hsdR-hsdM-hsdS* genes. (a) EOP experiments with crRNA targeting *ral* in *E. coli* BW25113 (methods). (b) EOP experiments with crRNA targeting *ral* in *E. coli* MG1655 that has an active type I restriction modification system. (c) EOP experiments with crRNA targeting *ral* in *E. coli* C3000 that has an active type I restriction modification system. For comparison, phage plaques appearing on *E. coli* lawn expressing a crRNA targeting essential gene *P* and nontargeting crRNA (targets P1 phage *mcp*) as a control are shown for lambda phage (Ctrl).

(TIF)

S3 Fig. CRISPRi of Nin region without and with plasmid expression gene Q: EOP experiments for assessing CRISPRi polarity effect on Nin region. (A) EOP for CRISPRi assay for each gene shown (each strain with individual CRISPRi plasmid (Methods)). (B) EOP experiments in presence of plasmids pQ and CRISPRi targeting each gene in Nin region context. We used the BW25113 strain with a crRNA vector control (DP51, crRNA targets P1 phage *mcp*) for estimating EOP.

(TIF)

S4 Fig. P1 phage genome, CRISPRi oligo designs. Blue represents genes, red represents primers, and black is the full genome. Outside is on the positive strand, where inside is negative.

(TIF)

S1 Table. List of bacterial strains and phages.

(XLSX)

S2 Table. List of primers used in this work.

(XLSX)

S3 Table. List of plasmids used in this work.

(XLSX)

S1 Text. Detailed discussion on phage CRISPRi results.

(DOCX)

S1 Data. The underlying data for all figures.

(XLSX)

Acknowledgments

The authors thank Dr. Jennifer Doudna (Innovative Genomics Institute, UC Berkeley) for sharing reagents and guidance. The authors also thank Dr. Benjamin Adler (Innovative Genomics Institute, UC Berkeley) for comments on the early draft of this manuscript.

Author Contributions

Conceptualization: Denish Piya, Vivek K. Mutalik.

Data curation: Denish Piya, Ry Young, Adam P. Arkin, Vivek K. Mutalik.

Formal analysis: Denish Piya, Vivek K. Mutalik.

Funding acquisition: Adam P. Arkin, Vivek K. Mutalik.

Investigation: Denish Piya, Nicholas Nolan, Madeline L. Moore, Luis A. Ramirez Hernandez, Vivek K. Mutalik.

Methodology: Denish Piya, Nicholas Nolan, Luis A. Ramirez Hernandez, Brady F. Cress, Ry Young, Vivek K. Mutalik.

Project administration: Vivek K. Mutalik.

Resources: Brady F. Cress, Ry Young, Adam P. Arkin, Vivek K. Mutalik.

Software: Nicholas Nolan, Vivek K. Mutalik.

Supervision: Adam P. Arkin, Vivek K. Mutalik.

Validation: Denish Piya, Vivek K. Mutalik.

Visualization: Vivek K. Mutalik.

Writing – original draft: Denish Piya, Vivek K. Mutalik.

Writing – review & editing: Brady F. Cress, Ry Young, Adam P. Arkin, Vivek K. Mutalik.

References

1. Breitbart M, Bonnain C, Malki K, Sawaya NA. Phage puppet masters of the marine microbial realm. *Nat Microbiol*. 2018; 3:754–766. <https://doi.org/10.1038/s41564-018-0166-y> PMID: 29867096
2. Suttle CA. Marine viruses—major players in the global ecosystem. *Nat Rev Microbiol*. 2007; 5:801–812. <https://doi.org/10.1038/nrmicro1750> PMID: 17853907
3. Koskella B, Hernandez CA, Wheatley RM. Understanding the Impacts of Bacteriophage Viruses: From Laboratory Evolution to Natural Ecosystems. *Annu Rev Virol*. 2022; 9:57–78. <https://doi.org/10.1146/annurev-virology-091919-075914> PMID: 35584889
4. Chevallereau A, Pons BJ, van Houte S, Westra ER. Interactions between bacterial and phage communities in natural environments. *Nat Rev Microbiol*. 2022; 20:49–62. <https://doi.org/10.1038/s41579-021-00602-y> PMID: 34373631
5. Correa AMS, Howard-Varona C, Coy SR, Buchan A, Sullivan MB, Weitz JS. Revisiting the rules of life for viruses of microorganisms. *Nat Rev Microbiol*. 2021; 19:501–513. <https://doi.org/10.1038/s41579-021-00530-x> PMID: 33762712
6. Roux S, Krupovic M, Daly RA, Borges AL, Nayfach S, Schulz F, et al. Cryptic inoviruses revealed as pervasive in bacteria and archaea across Earth's biomes. *Nat Microbiol*. 2019; 4:1895–1906. <https://doi.org/10.1038/s41564-019-0510-x> PMID: 31332386
7. Dominguez-Huerta G, Zayed AA, Wainaina JM, Guo J, Tian F, Pratama AA, et al. Diversity and ecological footprint of Global Ocean RNA viruses. *Science*. 2022; 376:1202–1208. <https://doi.org/10.1126/science.abn6358> PMID: 35679415
8. Neri U, Wolf YI, Roux S, Camargo AP, Lee B, Kazlauskas D, et al. Expansion of the global RNA virome reveals diverse clades of bacteriophages. *Cell*. 2022; 185:4023–4037.e18. <https://doi.org/10.1016/j.cell.2022.08.023> PMID: 36174579
9. Nayfach S, Páez-Espino D, Call L, Low SJ, Sberro H, Ivanova NN, et al. Metagenomic compendium of 189,680 DNA viruses from the human gut microbiome. *Nat Microbiol*. 2021; 6:960–970. <https://doi.org/10.1038/s41564-021-00928-6> PMID: 34168315
10. Hatfull GF. Actinobacteriophages: Genomics, Dynamics, and Applications. *Annu Rev Virol*. 2020; 7:37–61. <https://doi.org/10.1146/annurev-virology-122019-070009> PMID: 32991269
11. Fremin BJ, Bhatt AS, Kyrpides NC. Global Phage Small Open Reading Frame (GP-SmORF) Consortium. Thousands of small, novel genes predicted in global phage genomes. *Cell Rep*. 2022; 39:110984. <https://doi.org/10.1016/j.celrep.2022.110984> PMID: 35732113
12. Roux S, Emerson JB. Diversity in the soil virosphere: to infinity and beyond? *Trends Microbiol*. 2022; 30:1025–1035. <https://doi.org/10.1016/j.tim.2022.05.003> PMID: 35644779
13. Strathdee SA, Hatfull GF, Mutalik VK, Schooley RT. Phage therapy: From biological mechanisms to future directions. *Cell*. 2023; 186:17–31. <https://doi.org/10.1016/j.cell.2022.11.017> PMID: 36608652
14. Mutalik VK, Arkin AP. A Phage Foundry Framework to Systematically Develop Viral Countermeasures to Combat Antibiotic-Resistant Bacterial Pathogens. *iScience*. 2022; 25:104121. <https://doi.org/10.1016/j.isci.2022.104121> PMID: 35402883
15. Miller ES, Kutter E, Mosig G, Arisaka F, Kunisawa T, Rüger W. Bacteriophage T4 genome. *Microbiol Mol Biol Rev*. 2003; 67:86–156. table of contents. <https://doi.org/10.1128/MMBR.67.1.86-156.2003> PMID: 12626685
16. Dutilh BE, Reyes A, Hall RJ, Whiteson KL. Editorial: Virus Discovery by Metagenomics: The (Im)possibilities. *Front Microbiol*. 2017; 8:1710. <https://doi.org/10.3389/fmicb.2017.01710> PMID: 28943867
17. Casjens SR, Hendrix RW. Bacteriophage lambda: Early pioneer and still relevant. *Virology*. 2015; 479–480:310–330. <https://doi.org/10.1016/j.virol.2015.02.010> PMID: 25742714
18. Molineux I. T7 Bacteriophages. *Encyclopedia of Molecular Biology*. 2002. <https://doi.org/10.1002/047120918x.emb1510>
19. Pires DP, Cleto S, Sillankorva S, Azeredo J, Lu TK. Genetically Engineered Phages: a Review of Advances over the Last Decade. *Microbiol Mol Biol Rev*. 2016; 80:523–543. <https://doi.org/10.1128/MMBR.00069-15> PMID: 27250768

20. Adler BA, Chamakura K, Carion H, Krog J, Deutschbauer AM, Young R, et al. Multicopy suppressor screens reveal convergent evolution of single-gene lysis proteins. *Nat Chem Biol.* 2023. <https://doi.org/10.1038/s41589-023-01269-7> PMID: 36805702
21. Silas S, Carion H, Makarova KS, Laderman E, Godinez DS, Johnson M, et al. Parallelized screening of virus accessory genes reveals diverse defense and counter-defense mechanisms. 2023. <https://doi.org/10.1101/2023.04.06.535777>
22. Marinelli LJ, Piuri M, Swigonova Z, Balachandran A, Oldfield LM, van Kessel JC, et al. BRED: a simple and powerful tool for constructing mutant and recombinant bacteriophage genomes. *PLoS ONE.* 2008; 3:e3957. <https://doi.org/10.1371/journal.pone.0003957> PMID: 19088849
23. Dedrick RM, Marinelli LJ, Newton GL, Pogliano K, Pogliano J, Hatfull GF. Functional requirements for bacteriophage growth: gene essentiality and expression in mycobacteriophage Giles. *Mol Microbiol.* 2013; 88:577–589. <https://doi.org/10.1111/mmi.12210> PMID: 23560716
24. Pires DP, Monteiro R, Mil-Homens D, Fialho A, Lu TK, Azeredo J, et al. aeruginosa synthetic phages with reduced genomes. *Sci Rep.* 2021; 11:2164.
25. Mahler M, Costa AR, van Beljouw SPB, Fineran PC, Brouns SJJ. Approaches for bacteriophage genome engineering. *Trends Biotechnol.* 2022. <https://doi.org/10.1016/j.tibtech.2022.08.008> PMID: 36117025
26. Mitsunaka S, Yamazaki K, Pramono AK, Ikeuchi M, Kitao T, Ohara N, et al. Synthetic engineering and biological containment of bacteriophages. *Proc Natl Acad Sci U S A.* 2022; 119:e2206739119. <https://doi.org/10.1073/pnas.2206739119> PMID: 36409909
27. Meile S, Du J, Dunne M, Kilcher S, Loessner MJ. Engineering therapeutic phages for enhanced anti-bacterial efficacy. *Curr Opin Virol.* 2022; 52:182–191. <https://doi.org/10.1016/j.coviro.2021.12.003> PMID: 34952266
28. Yuan S, Shi J, Jiang J, Ma Y. Genome-scale top-down strategy to generate viable genome-reduced phages. *Nucleic Acids Res.* 2022; 50:13183–13197. <https://doi.org/10.1093/nar/gkac1168> PMID: 36511873
29. Adler BA, Hessler T, Cress BF, Lahiri A, Mutalik VK, Barrangou R, et al. Broad-spectrum CRISPR-Cas13a enables efficient phage genome editing. *Nat Microbiol.* 2022; 7:1967–1979. <https://doi.org/10.1038/s41564-022-01258-x> PMID: 36316451
30. Wetzel KS, Guerrero-Bustamante CA, Dedrick RM, Ko C-C, Freeman KG, Aull HG, et al. CRISPY-BRED and CRISPY-BRIP: efficient bacteriophage engineering. *Sci Rep.* 2021; 11:6796. <https://doi.org/10.1038/s41598-021-86112-6> PMID: 33762639
31. Guan J, Oromi-Bosch A, Mendoza SD, Karambelkar S, Berry JD, Bondy-Denomy J. Bacteriophage genome engineering with CRISPR-Cas13a. *Nat Microbiol.* 2022; 7:1956–1966. <https://doi.org/10.1038/s41564-022-01243-4> PMID: 36316452
32. Nethery MA, Hidalgo-Cantabrana C, Roberts A, Barrangou R. CRISPR-based engineering of phages for in situ bacterial base editing. *Proc Natl Acad Sci U S A.* 2022; 119:e2206744119. <https://doi.org/10.1073/pnas.2206744119> PMID: 36343261
33. Oechslein F, Zhu X, Dion MB, Shi R, Moineau S. Phage endolysins are adapted to specific hosts and are evolutionarily dynamic. *PLoS Biol.* 2022; 20:e3001740. <https://doi.org/10.1371/journal.pbio.3001740> PMID: 35913996
34. Bock C, Datlinger P, Chardon F, Coelho MA, Dong MB, Lawson KA, et al. High-content CRISPR screening. *Nat Rev Methods Primers.* 2022; 2:1–23. <https://doi.org/10.1038/s43586-022-00098-7> PMID: 37214176
35. Przybyla L, Gilbert LA. A new era in functional genomics screens. *Nat Rev Genet.* 2022; 23:89–103. <https://doi.org/10.1038/s41576-021-00409-w> PMID: 34545248
36. Qi LS, Larson MH, Gilbert LA, Doudna JA, Weissman JS, Arkin AP, et al. Repurposing CRISPR as an RNA-guided platform for sequence-specific control of gene expression. *Cell.* 2013; 152:1173–1183. <https://doi.org/10.1016/j.cell.2013.02.022> PMID: 23452860
37. Bikard D, Jiang W, Samai P, Hochschild A, Zhang F, Marraffini LA. Programmable repression and activation of bacterial gene expression using an engineered CRISPR-Cas system. *Nucleic Acids Res.* 2013; 41:7429–7437. <https://doi.org/10.1093/nar/gkt520> PMID: 23761437
38. Zhang X, Wang J, Cheng Q, Zheng X, Zhao G, Wang J. Multiplex gene regulation by CRISPR-ddCpf1. *Cell Discov.* 2017; 3:17018. <https://doi.org/10.1038/celldisc.2017.18> PMID: 28607761
39. Kim SK, Kim H, Ahn W-C, Park K-H, Woo E-J, Lee D-H, et al. Efficient transcriptional gene repression by type V-A CRISPR-Cpf1 from *Eubacterium eligens*. *ACS Synth Biol.* 2017; 6:1273–1282. <https://doi.org/10.1021/acssynbio.6b00368> PMID: 28375596

40. Specht DA, Xu Y, Lambert G. Massively parallel CRISPRi assays reveal concealed thermodynamic determinants of dCas12a binding. *Proc Natl Acad Sci U S A*. 2020; 117:11274–11282. <https://doi.org/10.1073/pnas.1918685117> PMID: 32376630
41. Hein MY, Weissman JS. Functional single-cell genomics of human cytomegalovirus infection. *Nat Biotechnol*. 2022; 40:391–401. <https://doi.org/10.1038/s41587-021-01059-3> PMID: 34697476
42. Fleck N, Grundner C. A Cas12a-based CRISPR interference system for multigene regulation in mycobacteria. *J Biol Chem*. 2021; 297:100990. <https://doi.org/10.1016/j.jbc.2021.100990> PMID: 34298016
43. Li L, Wei K, Zheng G, Liu X, Chen S, Jiang W, et al. CRISPR-Cpf1-Assisted Multiplex Genome Editing and Transcriptional Repression in Streptomyces. *Appl Environ Microbiol*. 2018;84. <https://doi.org/10.1128/AEM.00827-18> PMID: 29980561
44. Choi SY, Woo HM. CRISPRi-dCas12a: A dCas12a-Mediated CRISPR Interference for Repression of Multiple Genes and Metabolic Engineering in Cyanobacteria. *ACS Synth Biol*. 2020; 9:2351–2361. <https://doi.org/10.1021/acssynbio.0c00091> PMID: 32379967
45. Liu Y, Dai L, Dong J, Chen C, Zhu J, Rao VB, et al. Covalent Modifications of the Bacteriophage Genome Confer a Degree of Resistance to Bacterial CRISPR Systems. *J Virol*. 2020;94. <https://doi.org/10.1128/JVI.01630-20> PMID: 32938767
46. Huang CJ, Adler BA, Doudna JA. A naturally DNase-free CRISPR-Cas12c enzyme silences gene expression. *Mol Cell*. 2022; 82:2148–2160.e4. <https://doi.org/10.1016/j.molcel.2022.04.020> PMID: 35659325
47. Wright BW, Molloy MP, Jaschke PR. Overlapping genes in natural and engineered genomes. *Nat Rev Genet*. 2022; 23:154–168. <https://doi.org/10.1038/s41576-021-00417-w> PMID: 34611352
48. Shcherbakov DV, Garber MB. [Overlapping genes in bacterial and bacteriophage genomes]. *Mol Biol*. 2000; 34:572–583.
49. Parent KN, Schrad JR, Cingolani G. Breaking Symmetry in Viral Icosahedral Capsids as Seen through the Lenses of X-ray Crystallography and Cryo-Electron Microscopy. *Viruses*. 2018;10. <https://doi.org/10.3390/v10020067> PMID: 29414851
50. Wikoff WR, Johnson JE. Virus assembly: Imaging a molecular machine. *Curr Biol*. 1999; 9:R296–R300. [https://doi.org/10.1016/s0960-9822\(99\)80183-3](https://doi.org/10.1016/s0960-9822(99)80183-3) PMID: 10226016
51. Leiman PG, Kanamaru S, Mesyanzhinov VV, Arisaka F, Rossmann MG. Structure and morphogenesis of bacteriophage T4. *Cell Mol Life Sci*. 2003; 60:2356–2370. <https://doi.org/10.1007/s00018-003-3072-1> PMID: 14625682
52. Lobočka MB, Rose DJ, Plunkett G 3rd, Rusin M, Samoedny A, Lehnerr H, et al. Genome of bacteriophage P1. *J Bacteriol*. 2004; 186:7032–7068. <https://doi.org/10.1128/JB.186.21.7032-7068.2004> PMID: 15489417
53. Knott GJ, Cress BF, Liu JJ, Thornton BW, Lew RJ, Al-Shayeb B, et al. Structural basis for AcrVA4 inhibition of specific CRISPR-Cas12a. *Elife*. 2019;8. <https://doi.org/10.7554/eLife.49110> PMID: 31397669
54. Piya DK. Interactions between host and phage encoded factors shape phage infection. Doctoral dissertation, Texas A & M University. 2018. Available from: <https://oaktrust.library.tamu.edu/handle/1969.1/174423>
55. Hendrix RW. *Lambda II*. Cold Spring Harbor Laboratory; 1983.
56. Toothman P, Herskowitz I. Rex-dependent exclusion of lambdoid phages. I. Prophage requirements for exclusion. *Virology*. 1980; 102:133–146. [https://doi.org/10.1016/0042-6822\(80\)90076-8](https://doi.org/10.1016/0042-6822(80)90076-8) PMID: 6445121
57. Gottesman ME, Yarmolinsky MB. The Integration and Excision of the Bacteriophage Lambda Genome. *Cold Spring Harb Symp Quant Biol*. 1968:735–747. <https://doi.org/10.1101/sqb.1968.033.01.084> PMID: 5254582
58. Caldwell BJ, Bell CE. Structure and mechanism of the Red recombination system of bacteriophage lambda. *Prog Biophys Mol Biol*. 2019; 147:33–46.
59. Haeusser DP, Hoashi M, Weaver A, Brown N, Pan J, Sawitzke JA, et al. The Kil peptide of bacteriophage lambda blocks *Escherichia coli* cytokinesis via ZipA-dependent inhibition of FtsZ assembly. *PLoS Genet*. 2014; 10:e1004217.
60. Zabeau M, Friedman S, Van Montagu M, Schell J. The *ral* gene of phage lambda. I. Identification of a non-essential gene that modulates restriction and modification in *E. coli*. *Mol Gen Genet*. 1980; 179:63–73. <https://doi.org/10.1007/BF00268447> PMID: 6256607
61. Debrouwere L, Zabeau M, Van Montagu M, Schell J. The *ral* gene of phage lambda. II. Isolation and characterization of *ral* deficient mutants. *Mol Gen Genet*. 1980; 179:75–80. <https://doi.org/10.1007/BF00268448> PMID: 6256608

62. Hendrix RW, Duda RL. Bacteriophage lambda PaPa: not the mother of all lambda phages. *Science*. 1992; 258:1145–1148. <https://doi.org/10.1126/science.1439823> PMID: 1439823
63. Cheng SW, Court DL, Friedman DI. Transcription termination signals in the nin region of bacteriophage lambda: identification of Rho-dependent termination regions. *Genetics*. 1995; 140:875–887. <https://doi.org/10.1093/genetics/140.3.875> PMID: 7672588
64. Kroger M, Hobom G. A chain of interlinked genes in the nin R region of bacteriophage lambda. *Gene*. 1982; 20:25–38. [https://doi.org/10.1016/0378-1119\(82\)90084-1](https://doi.org/10.1016/0378-1119(82)90084-1) PMID: 6219042
65. Court D, Sato K. Studies of novel transducing variants of lambda: dispensability of genes N and Q. *Virology*. 1969; 39:348–352. [https://doi.org/10.1016/0042-6822\(69\)90060-9](https://doi.org/10.1016/0042-6822(69)90060-9) PMID: 5344297
66. Rousset F, Cui L, Siouve E, Becavin C, Depardieu F, Bikard D. Genome-wide CRISPR-dCas9 screens in *E. coli* identify essential genes and phage host factors. *PLoS Genet*. 2018; 14:e1007749. <https://doi.org/10.1371/journal.pgen.1007749> PMID: 30403660
67. Liu X, Gallay C, Kjos M, Domenech A, Slager J, Kessel SP, et al. High-throughput CRISPRi phenotyping identifies new essential genes in *Streptococcus pneumoniae*. *Mol Syst Biol*. 2017; 13:931. <https://doi.org/10.15252/msb.20167449> PMID: 28490437
68. Peters JM, Colavin A, Shi H, Czarny TL, Larson MH, Wong S, et al. A Comprehensive, CRISPR-based Functional Analysis of Essential Genes in Bacteria. *Cell*. 2016; 165:1493–1506. <https://doi.org/10.1016/j.cell.2016.05.003> PMID: 27238023
69. Wang T, Guan C, Guo J, Liu B, Wu Y, Xie Z, et al. Pooled CRISPR interference screening enables genome-scale functional genomics study in bacteria with superior performance. *Nat Commun*. 2018; 9:2475. <https://doi.org/10.1038/s41467-018-04899-x> PMID: 29946130
70. Rishi HS, Toro E, Liu H, Wang X, Qi LS, Arkin AP. Systematic genome-wide querying of coding and non-coding functional elements in *E. coli* using CRISPRi. *bioRxiv*. 2020. p. 2020.03.04.975888. <https://doi.org/10.1101/2020.03.04.975888>
71. Friedman DI, Court DL. Transcription antitermination: the lambda paradigm updated. *Mol Microbiol*. 1995; 18:191–200. https://doi.org/10.1111/j.1365-2958.1995.mmj_18020191.x PMID: 8709839
72. Gründling A, Manson MD, Young R. Holins kill without warning. *Proc Natl Acad Sci U S A*. 2001; 98:9348–9352. <https://doi.org/10.1073/pnas.151247598> PMID: 11459934
73. Gonzales MF, Piya DK, Koehler B, Zhang K, Yu Z, Zeng L, et al. New Insights into the Structure and Assembly of Bacteriophage P1. *Viruses*. 2022;14. <https://doi.org/10.3390/v14040678> PMID: 35458408
74. Windle BE, Laufer CS, Hays JB. Sequence and deletion analysis of the recombination enhancement gene (ref) of bacteriophage P1: evidence for promoter-operator and attenuator-antiterminator control. *J Bacteriol*. 1988; 170:4881–4889. <https://doi.org/10.1128/jb.170.10.4881-4889.1988> PMID: 3170487
75. Wetmore KM, Price MN, Waters RJ, Lamson JS, He J, Hoover CA, et al. Rapid quantification of mutant fitness in diverse bacteria by sequencing randomly bar-coded transposons. *MBio*. 2015; 6:e00306–e00315. <https://doi.org/10.1128/mBio.00306-15> PMID: 25968644
76. Mutalik VK, Adler BA, Rishi HS, Piya D, Zhong C, Koskella B, et al. High-throughput mapping of the phage resistance landscape in *E. coli*. *PLoS Biol*. 2020; 18:e3000877. <https://doi.org/10.1371/journal.pbio.3000877> PMID: 33048924
77. Jiang W, Oikonomou P, Tavazoie S. Comprehensive Genome-wide Perturbations via CRISPR Adaptation Reveal Complex Genetics of Antibiotic Sensitivity. *Cell*. 2020; 180:1002–1017.e31. <https://doi.org/10.1016/j.cell.2020.02.007> PMID: 32109417
78. Liu X, Jiang H, Gu Z, Roberts JW. High-resolution view of bacteriophage lambda gene expression by ribosome profiling. *Proc Natl Acad Sci U S A*. 2013; 110:11928–11933. <https://doi.org/10.1073/pnas.1309739110> PMID: 23812753
79. Hall PM, Inman JT, Fulbright RM, Le TT, Brewer JJ, Lambert G, et al. Polarity of the CRISPR roadblock to transcription. *Nat Struct Mol Biol*. 2022; 29:1217–1227. <https://doi.org/10.1038/s41594-022-00864-x> PMID: 36471058
80. Adler BA, Al-Shimary MJ, Patel JR, Armbruster E, Colognori D, Charles EJ, et al. Genome-wide Characterization of Diverse Bacteriophages Enabled by RNA-Binding CRISPRi. *bioRxiv*. 2023: p. 2023.09.18.558157. <https://doi.org/10.1101/2023.09.18.558157>
81. Carlson HK, Piya D, Moore ML, Magar RT, Elisabeth NH, Deutschbauer AM, et al. Geochemical constraints on bacteriophage infectivity in terrestrial environments. *bioRxiv*. 2023. p. 2023.04.10.536276. <https://doi.org/10.1038/s43705-023-00297-7> PMID: 37596312
82. Wang JY, Doudna JA. CRISPR technology: A decade of genome editing is only the beginning. *Science*. 2023; 379:eadd8643. <https://doi.org/10.1126/science.add8643> PMID: 36656942
83. Adams MH. Bacteriophages. New York, NY: Interscience Publishers; 1959.

84. Pryor JM, Potapov V, Kucera RB, Bilotti K, Cantor EJ, Lohman GJS. Enabling one-pot Golden Gate assemblies of unprecedented complexity using data-optimized assembly design. *PLoS ONE*. 2020; 15:e0238592. <https://doi.org/10.1371/journal.pone.0238592> PMID: 32877448
85. Guzman LM, Belin D, Carson MJ, Beckwith J. Tight regulation, modulation, and high-level expression by vectors containing the arabinose P_{BAD} promoter. *J Bacteriol*. 1995; 177:4121–4130.
86. Bari SMN, Walker FC, Cater K, Aslan B, Hatoum-Aslan A. Strategies for Editing Virulent Staphylococcal Phages Using CRISPR-Cas10. *ACS Synth Biol*. 2017; 6:2316–2325. <https://doi.org/10.1021/acssynbio.7b00240> PMID: 28885820
87. Gibson DG, Young L, Chuang RY, Venter JC, Hutchison CA 3rd, Smith HO. Enzymatic assembly of DNA molecules up to several hundred kilobases. *Nat Methods*. 2009; 6:343–345. <https://doi.org/10.1038/nmeth.1318> PMID: 19363495
88. Chung CT, Niemela SL, Miller RH. One-step preparation of competent *Escherichia coli*: transformation and storage of bacterial cells in the same solution. *Proc Natl Acad Sci U S A*. 1989; 86:2172–2175. <https://doi.org/10.1073/pnas.86.7.2172> PMID: 2648393
89. Hupfeld M, Trasanidou D, Ramazzini L, Klumpp J, Loessner MJ, Kilcher S. A functional type II-A CRISPR-Cas system from *Listeria* enables efficient genome editing of large non-integrating bacteriophage. *Nucleic Acids Res*. 2018; 46:6920–6933. <https://doi.org/10.1093/nar/gky544> PMID: 30053228
90. Price MN, Ray J, Iavarone AT, Carlson HK, Ryan EM, Malmstrom RR, et al. Oxidative Pathways of Deoxyribose and Deoxyribonate Catabolism. *mSystems*. 2019;4. <https://doi.org/10.1128/mSystems.00297-18> PMID: 30746495
91. Weisberg RA, Sternberg N, Gallay E. The nu1 gene of coliphage lambda. *Virology*. 1979; 95:99–106. [https://doi.org/10.1016/0042-6822\(79\)90404-5](https://doi.org/10.1016/0042-6822(79)90404-5) PMID: 442547
92. Harrison DP, Brown DT, Bode VC. The lambda head-tail joining reaction: purification, properties and structure of biologically active heads and tails. *J Mol Biol*. 1973; 79:437–449. [https://doi.org/10.1016/0022-2836\(73\)90397-5](https://doi.org/10.1016/0022-2836(73)90397-5) PMID: 4202216
93. Kaiser D, Syvanen M, Masuda T. Processing and assembly of the head of bacteriophage lambda. *J Supramol Struct*. 1974; 2:318–328. <https://doi.org/10.1002/jss.400020221> PMID: 4437179
94. Boklage CE, Wong EC, Bode VC. Functional abnormality of lambda phage particles from complemented FII-mutant lysates. *Virology*. 1974; 61:22–28. [https://doi.org/10.1016/0042-6822\(74\)90238-4](https://doi.org/10.1016/0042-6822(74)90238-4) PMID: 4413519
95. Medina E, Wieczorek D, Medina EM, Yang Q, Feiss M, Catalano CE. Assembly and maturation of the bacteriophage lambda procapsid: gpC is the viral protease. *J Mol Biol*. 2010; 401:813–830. <https://doi.org/10.1016/j.jmb.2010.06.060> PMID: 20620152
96. Ray P, Murialdo H. The role of gene Nu3 in bacteriophage lambda head morphogenesis. *Virology*. 1975; 64:247–263. [https://doi.org/10.1016/0042-6822\(75\)90096-3](https://doi.org/10.1016/0042-6822(75)90096-3) PMID: 1090075
97. Hohn B, Hohn T. Activity of empty, headlike particles for packaging of DNA of bacteriophage lambda in vitro. *Proc Natl Acad Sci U S A*. 1974; 71:2372–2376. <https://doi.org/10.1073/pnas.71.6.2372> PMID: 4601587
98. Catalano CE, Tomka MA. Role of gpFI protein in DNA packaging by bacteriophage lambda. *Biochemistry*. 1995; 34:10036–10042. <https://doi.org/10.1021/bi00031a027> PMID: 7632676
99. Kemp CL, Howatson AF, Siminovitich L. Electron microscopy studies of mutants of lambda bacteriophage. I. General description and quantitation of viral products. *Virology*. 1968; 36:490–502. [https://doi.org/10.1016/0042-6822\(68\)90174-8](https://doi.org/10.1016/0042-6822(68)90174-8) PMID: 4881034
100. Szybalski EH, Szybalski W. A comprehensive molecular map of bacteriophage lambda. *Gene*. 1979; 7:217–270. [https://doi.org/10.1016/0378-1119\(79\)90047-7](https://doi.org/10.1016/0378-1119(79)90047-7) PMID: 160360
101. Enquist LW, Skalka A. Replication of bacteriophage lambda DNA dependent on the function of host and viral genes. I. Interaction of red, gam and rec. *J Mol Biol*. 1973; 75:185–212. [https://doi.org/10.1016/0022-2836\(73\)90016-8](https://doi.org/10.1016/0022-2836(73)90016-8) PMID: 4580674
102. Greer H. The kil gene of bacteriophage lambda. *Virology*. 1975; 66:589–604. [https://doi.org/10.1016/0042-6822\(75\)90231-7](https://doi.org/10.1016/0042-6822(75)90231-7) PMID: 1098278
103. Kaiser AD. Mutations in a temperate bacteriophage affecting its ability to lysogenize *Escherichia coli*. *Virology*. 1957; 3:42–61. [https://doi.org/10.1016/0042-6822\(57\)90022-3](https://doi.org/10.1016/0042-6822(57)90022-3) PMID: 13409759
104. Truitt CL, Chu H, Walker JR. Bacteriophage lambda mutants (lambda_{datp}) that overproduce repressor. *J Virol*. 1978; 28:877–884.
105. Campbell A. Comparative molecular biology of lambda_{doid} phages. *Annu Rev Microbiol*. 1994; 48:193–222. <https://doi.org/10.1146/annurev.mi.48.100194.001205> PMID: 7826005
106. Radding CM. Nuclease activity in defective lysogens of phage lambda. *Biochem Biophys Res Commun*. 1964; 15:8–12. [https://doi.org/10.1016/0006-291x\(64\)90093-2](https://doi.org/10.1016/0006-291x(64)90093-2) PMID: 5319710

107. Galland P, Cortini R, Calef E. Control of gene expression in bacteriophage lambda: suppression of N mutants by mutations of the antirepressor. *Mol Gen Genet.* 1975; 142:155–170. <https://doi.org/10.1007/BF00266096> PMID: 765738
108. Thomas R, Lambert L. On the occurrence of bacterial mutations permitting lysogenization by clear variants of temperate bacteriophages. *J Mol Biol.* 1962; 5:373–374. [https://doi.org/10.1016/s0022-2836\(62\)80079-5](https://doi.org/10.1016/s0022-2836(62)80079-5) PMID: 13981108
109. Lieb M. Mapping missense and nonsense mutation in gene *cl* of bacteriophage lambda: marker effects. *Mol Gen Genet.* 1976; 146:285–290. <https://doi.org/10.1007/BF00701252> PMID: 794694
110. Eisen H, Brachet P, Pereira da Silva L, Jacob F. Regulation of repressor expression in lambda. *Proc Natl Acad Sci U S A.* 1970; 66:855–862. <https://doi.org/10.1073/pnas.66.3.855> PMID: 5269249
111. Kleckner N. Amber mutants in the O gene of bacteriophage lambda are not efficiently complemented in the absence of phage N function. *Virology.* 1977; 79:174–182. [https://doi.org/10.1016/0042-6822\(77\)90343-9](https://doi.org/10.1016/0042-6822(77)90343-9) PMID: 325882
112. Mukai T, Ohkubo H, Shimada K, Takagi Y. Isolation and characterization of a plaque-forming lambda bacteriophage carrying a ColE1 plasmid. *J Bacteriol.* 1978; 135:171–177. <https://doi.org/10.1128/jb.135.1.171-177.1978> PMID: 670149
113. Tarkowski TA, Mooney D, Thomason LC, Stahl FW. Gene products encoded in the *ninR* region of phage lambda participate in Red-mediated recombination. *Genes Cells.* 2002; 7:351–363. <https://doi.org/10.1046/j.1365-2443.2002.00531.x> PMID: 11952832
114. Chang CY, Nam K, Young R. S gene expression and the timing of lysis by bacteriophage lambda. *J Bacteriol.* 1995; 177:3283–3294. <https://doi.org/10.1128/jb.177.11.3283-3294.1995> PMID: 7768829
115. Young R. Phage lysis: three steps, three choices, one outcome. *J Microbiol.* 2014; 52:243–258. <https://doi.org/10.1007/s12275-014-4087-z> PMID: 24585055
116. Zhang N, Young R. Complementation and characterization of the nested Rz and Rz1 reading frames in the genome of bacteriophage lambda. *Mol Gen Genet.* 1999; 262:659–667. <https://doi.org/10.1007/s004380051128> PMID: 10628848
117. Sternberg N, Sauer B, Hoess R, Abremski K. Bacteriophage P1 cre gene and its regulatory region. Evidence for multiple promoters and for regulation by DNA methylation. *J Mol Biol.* 1986; 187:197–212. [https://doi.org/10.1016/0022-2836\(86\)90228-7](https://doi.org/10.1016/0022-2836(86)90228-7) PMID: 3486297
118. Lu SD, Lu D, Gottesman M. Stimulation of IS1 excision by bacteriophage P1 ref function. *J Bacteriol.* 1989; 171:3427–3432. <https://doi.org/10.1128/jb.171.6.3427-3432.1989> PMID: 2542224
119. Lehnher H, Jensen CD, Stenholm AR, Dueholm A. Dual regulatory control of a particle maturation function of bacteriophage P1. *J Bacteriol.* 2001; 183:4105–4109. <https://doi.org/10.1128/JB.183.14.4105-4109.2001> PMID: 11418548
120. Iida S, Meyer J, Bachi B, Stalhammar-Carlemalm M, Schrickel S, Bickle TA, et al. DNA restriction—modification genes of phage P1 and plasmid p15B. Structure and in vitro transcription. *J Mol Biol.* 1983; 165:1–18. [https://doi.org/10.1016/s0022-2836\(83\)80239-3](https://doi.org/10.1016/s0022-2836(83)80239-3) PMID: 6302279
121. Schaefer TS, Hays JB. The *bof* gene of bacteriophage P1: DNA sequence and evidence for roles in regulation of phage *c1* and *ref* genes. *J Bacteriol.* 1990; 172:3269–3277. <https://doi.org/10.1128/jb.172.6.3269-3277.1990> PMID: 2345146
122. Piya D, Vara L, Russell WK, Young R, Gill JJ. The multicomponent antirestriction system of phage P1 is linked to capsid morphogenesis. *Mol Microbiol.* 2017; 105:399–412. <https://doi.org/10.1111/mmi.13705> PMID: 28509398
123. Schmidt C, Velleman M, Arber W. Three functions of bacteriophage P1 involved in cell lysis. *J Bacteriol.* 1996; 178:1099–1104. <https://doi.org/10.1128/jb.178.4.1099-1104.1996> PMID: 8576044
124. Iida S, Arber W. Plaque forming specialized transducing phage P1: isolation of P1CmSmSu, a precursor of P1Cm. *Mol Gen Genet.* 1977; 153:259–269. <https://doi.org/10.1007/BF00431591> PMID: 895711
125. Iida S, Meyer J, Kennedy KE, Arber W. A site-specific, conservative recombination system carried by bacteriophage P1. Mapping the recombinase gene *cin* and the cross-over sites *cix* for the inversion of the C segment. *EMBO J.* 1982; 1:1445–1453. <https://doi.org/10.1002/j.1460-2075.1982.tb01336.x> PMID: 6327269
126. Iida S. Bacteriophage P1 carries two related sets of genes determining its host range in the invertible C segment of its genome. *Virology.* 1984; 134:421–434. [https://doi.org/10.1016/0042-6822\(84\)90309-x](https://doi.org/10.1016/0042-6822(84)90309-x) PMID: 6100576
127. Guidolin A, Zingg JM, Arber W. Organization of the bacteriophage P1 tail-fibre operon. *Gene.* 1989; 76:239–243. [https://doi.org/10.1016/0378-1119\(89\)90164-9](https://doi.org/10.1016/0378-1119(89)90164-9) PMID: 2526777
128. Walker JT, Walker DH Jr. Coliphage P1 morphogenesis: analysis of mutants by electron microscopy. *J Virol.* 1983; 45:1118–1139. <https://doi.org/10.1128/JVI.45.3.1118-1139.1983> PMID: 6834479

129. Devlin BH, Baumstark BR, Scott JR. Superimmunity: characterization of a new gene in the immunity region of P1. *Virology*. 1982; 120:360–375. [https://doi.org/10.1016/0042-6822\(82\)90037-x](https://doi.org/10.1016/0042-6822(82)90037-x) PMID: 6285609
130. Heinrich J, Citron M, Gunther A, Schuster H. Second-site suppressors of the bacteriophage P1 virs mutant reveal the interdependence of the c4, icd, and ant genes in the P1 imm1 operon. *J Bacteriol*. 1994; 176:4931–4936. <https://doi.org/10.1128/jb.176.16.4931-4936.1994> PMID: 8051007
131. Hansen EB. Structure and regulation of the lytic replicon of phage P1. *J Mol Biol*. 1989; 207:135–149. [https://doi.org/10.1016/0022-2836\(89\)90445-2](https://doi.org/10.1016/0022-2836(89)90445-2) PMID: 2661831
132. Coulby JN, Sternberg NL. Characterization of the phage P1 dam gene. *Gene*. 1988; 74:191. [https://doi.org/10.1016/0378-1119\(88\)90284-3](https://doi.org/10.1016/0378-1119(88)90284-3) PMID: 3248723
133. D'Ari R, Jaffe-Brachet A, Touati-Schwartz D, Yarmolinsky MB. A dnaB analog specified by bacteriophage P1. *J Mol Biol*. 1975; 94:341–366. [https://doi.org/10.1016/0022-2836\(75\)90207-7](https://doi.org/10.1016/0022-2836(75)90207-7) PMID: 1100840
134. Lehnher H, Guidolin A, Arber W. Bacteriophage P1 gene 10 encodes a trans-activating factor required for late gene expression. *J Bacteriol*. 1991; 173:6438–6445. <https://doi.org/10.1128/jb.173.20.6438-6445.1991> PMID: 1917870
135. Skorupski K, Pierce JC, Sauer B, Sternberg N. Bacteriophage P1 genes involved in the recognition and cleavage of the phage packaging site (pac). *J Mol Biol*. 1992; 223:977–989. [https://doi.org/10.1016/0022-2836\(92\)90256-j](https://doi.org/10.1016/0022-2836(92)90256-j) PMID: 1538406
136. Baumstark BR, Stovall SR, Bralley P. The ImmC region of phage P1 codes for a gene whose product promotes lytic growth. *Virology*. 1990; 179:217–227. [https://doi.org/10.1016/0042-6822\(90\)90291-x](https://doi.org/10.1016/0042-6822(90)90291-x) PMID: 2120849